

MODELING AND SIMULATION OF THE SWITCHED RELUCTANCE MOTOR

by

RAHEEL AHMED SHAIKH

**Progress Report submitted in partial fulfilment of
the requirements for the
Bachelor of Engineering (Hons)
(Electrical & Electronics Engineering)**

MAY 2011

**Universiti Teknologi PETRONAS
Bandar Seri Iskandar
31750 Tronoh
Perak Darul Ridzuan**

© Copyright 2011

by

Raheel Ahmed Shaikh

CERTIFICATION OF APPROVAL

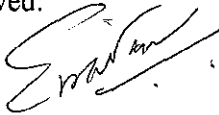
MODELING AND SIMULATION OF THE SWITCHED RELUCTANCE MOTOR

by

Raheel Ahmed Shaikh

A project dissertation submitted to the
Electrical & Electronics Engineering Programme
Universiti Teknologi PETRONAS
in partial fulfilment of the requirement for the
Bachelor of Engineering (Hons)
(Electrical & Electronics Engineering)

Approved:



Dr. Irraivan Elamvazuthi

Project supervisor

UNIVERSITI TEKNOLOGI PETRONAS
TRONOH, PERAK
MAY 2011

CERTIFICATION OF ORIGINALITY

This project is to certify that I am responsible for the work submitted in this project, that the original work is my own except as specified in the reference and acknowledgments, and that the original work contained herein have not been undertaken or done by un specified sources or persons.

A handwritten signature in black ink, appearing to read 'Raheel', with a long horizontal flourish underneath.

Raheel Ahmed Shaikh

ABSTRACT

This Paper summarizes the study conducted on the techniques used and implemented to minimize the torque ripple of the Switched reluctance Motors. These motors although offering the advantages of higher speeds, reliability and phase independence, have the limitations of the torque ripple and non-linearity in the magnetic characteristics. Thus in order to have the good understanding of the Motor, it is simulated in the MATLAB/SIMULINK environment. This paper describes details on modeling of two different configurations of Switched Reluctance Motor concentrating only on the linear model by obeying all of its characteristics. The two configurations of motors are applied with two different control techniques and the results are calculated and tabulated. Load and No load analysis are also performed to understand the behavior of motor with load. Through out the analysis, various values of turn-on and turn-off angles are selected and finally the optimum values are calculated based on the performance parameters of Average torque, speed and torque ripple. All simulations are documented through this paper including its block models and initializations performed. Finally a control technique is recommended which produces the best results with smallest torque ripple.

ACKNOWLEDGEMENT

First of all, I would like to thank the almighty god, who gave me the discipline and courage to finish this project. Without his blessings, the project might not have been completed. I would also like to thank both my parents for their encouragements and prayers. Without their support it would have been difficult to finish this project

Next, I would like to convey my deepest appreciation towards my final year project supervisor, Dr. **Irraivan Elamvazuthi**, who has persistently and determinedly assisted me during the project. It would have been very arduous to complete this project without the passionate supports and guidance encouragement and advices given by him.

Thirdly, I would like to thank to Universiti Teknologi PETRONAS (UTP) and Electrical Engineering for providing us theoretical knowledge which can be applied in our Final Year Project.

Lastly, I would love to thank the people that have been giving me morale support all the way through the time I was doing the project. Thank you.

TABLE OF CONTENTS

ABSTRACT.....	iv
ACKNOWLEDGEMENT	v
LIST OF FIGURES.....	viii
LIST OF TABLE.....	x
NOMENCLATURE & ACRONYMS	xi

CHAPTER 1: INTRODUCTION

1.1	Background of Study.....	1
1.2	Stepping Motors	3
1.3	Types of Stepping Motors.....	4
	1.3.1 Variable Reluctance Motor.....	4
	1.3.2 Permanent Magnet Motor.....	5
	1.3.3 Hybrid Motor.....	5
1.4	Problem Statement.....	7
1.5	Objectives of the Study.....	7
1.6	Scope of Study.....	8

CHAPTER 2: LITERATURE REVIEW

2.1	Previous Work Done.....	9
	2.1.1 Techniques & Algorithms Applied.....	10
2.2	Variable Reluctance Motor.....	11
	2.2.1 Advantages & Disadvantages.....	11
	2.2.2 Construction.....	12
	2.2.3 Operation.....	12
	2.2.4 Energy Conversion Principles of SRM.....	13
	2.2.5 Basic Control Circuit.....	16
	2.4.6 Torque Speed Characteristics	17

CHAPTER 3: METHODOLOGY

3.1	Project Flow.....	19
3.1.1	Phases Involved in Project Completion....	20
3.2	Tools & Software Required	21
3.3	Insight into SRM	22
3.3.1	SRM energizing strategies	27
3.3.2	Two quadrant chopping convertor.....	27
3.3.3	Selection of Stator and Rotor Pole arcs....	29
3.3.4	SRM modelling equations	30
3.3.5	Application Example.....	32

CHAPTER 4: RESULTS & DISCUSSION

4.1	Simulation of 6/4 SRM	39
4.1.1	Voltage Pulse technique with no load	45
4.1.2	Simulations with varied θ on and θ off...	49
4.1.3	Voltage Pulse with variable load	52
4.1.4	Simulation of motor with $\beta_r \neq \beta_s$	55
4.1.5	Varied θ on and θ off for $\beta_r \neq \beta_s$	57
4.1.6	Comparison between $\beta_r \neq \beta_s$ & $\beta_r = \beta_s$	61
4.1.7	Hysteresis Control with no load	62
4.2	Simulation of 8/6 SRM	70
4.2.1	Voltage Pulse technique with no load	72
4.2.2	Varied θ on and θ off for variable load ..	76

CHAPTER 5: CONCLUSION & RECOMMENDATIONS

5.1	Conclusion	79
5.2	Recommendations	80

REFERENCES	81
------------------	----

APPENDIX I: PROJECT GANTT CHART.....	
--------------------------------------	--

APPENDIX I: SIMULATION INITIALIZATIONS.....	
---	--

LIST OF FIGURES

Figure 1:	Classification of Motors.....	2
Figure 2:	Cross section of a Variable Reluctance Motor.....	4
Figure 3:	Components of Permanent Magnet Stepper Motor.....	5
Figure 4:	Hybrid Stepping Motor.....	6
Figure 5:	Variable Reluctance Stepper Motor.....	12
Figure 6:	Aligned Position of SRM	14
Figure 7:	Un-aligned Position of SRM	14
Figure 8:	Rotor Switching Sequence of VRM.....	15
Figure 9:	VRM Control Circuit.....	17
Figure 10:	SRM torque speed characteristics.....	17
Figure 11:	Variation of Inductance and Torque of one phase.....	23
Figure 12:	Two quadrant Chopping Convertor.....	27
Figure 13:	Switching of the Two quadrants Chopping Convertor.....	28
Figure 14:	Results produced as a result of two quadrant Chopping Convertor.	29
Figure 15:	Model of SRM available in MATLAB.....	32
Figure 16:	MATLAB blocks for the SRM simulation	35
Figure 17:	Converter Block	35
Figure 18:	Sub-converter Block	35
Figure 19:	Output of the SRM.....	36
Figure 20:	Output of the SRM at low speeds.....	37
Figure 21:	Mechanical equation block diagram via SIMULINK.....	38
Figure 22:	Complete Simulation Model of 6/4 SRM	39
Figure 23:	Phase Model of SRM.....	40
Figure 24:	Modulo $\pi/2$ Model.....	41
Figure 25:	Switch Model.....	41
Figure 26:	Inductance Model.....	42
Figure 27:	Torque Model.....	43

Figure 28:	Different configurations implemented on 6/4 SRM.....	43
Figure 29:	Output of Total Torque, Speed and rotation of 6/4 Motor at No load.....	45
Figure 30:	(a) Individual Torques generated from each phase, (b) Expanded view of Individual Torques generated	46
Figure 31:	(a) Inductance profile of all the three phases, (b) voltage Pulses applied to three phases, (c) Current output of Phase A .	47
Figure 32:	(a) Total Torque, Speed and rotation with $\theta_{on}=7$ and $\theta_{off} = 33$, (b) Expanded view of the results simulated in (a).....	50
Figure 33:	Simulation of Voltage Pulses and current of Phase A.....	51
Figure 34:	(a) Voltage Pulses applied to three phases, (b) Current output of Phase A.....	55
Figure 35:	Inductance profile of all the three phases.....	56
Figure 36:	(a) Total Torque, Speed and rotation with $\theta_{on}=10$ and $\theta_{off} = 35$, (b) Expanded view of the results simulated in (a).....	58
Figure 37:	Voltage Pulses to individual phases and current of Phase A.....	59
Figure 38:	Inductance profile of each phase and Current produced in each phase.....	59
Figure 39:	Inductance, Current and Torque of Phase A.....	60
Figure 40:	(a) Torque Produced, Speed and Rotation (b) Expanded view of Torque and Speed.....	63
Figure 41:	(a) Expanded view of Voltage Pulses applied and Current Produced in Phase A, (b) Voltage pulses applied to all the phases, inductance of all phases and current produced.....	64
Figure 42:	Complete Simulation Model of 8/6 SRM.....	70
Figure 43:	Output of Total Torque, Speed and rotation of 8/6 Motor with little load.....	72
Figure 44:	(a) Expanded view of Individual Torques generated from each phase, (b) Individual Phase Inductances	73
Figure 45:	(a) Expanded view of Individual Voltage Pulses Applied, (b) Voltage Pulses, Phase Inductances and Phase Currents produced.....	74
Figure 46:	Hysteresis control of SRM.....	78

1.3 Types of Stepping Motors [9]

There are three basic types of stepping motors: permanent magnet, variable reluctance and hybrid. Permanent magnet motors have a magnetized rotor, while variable reluctance motors have toothed soft-iron rotors. Hybrid stepping motors combine aspects of both permanent magnet and variable reluctance technology. The stator or stationary part of the stepping motor holds multiple windings. The arrangement of these windings is the primary factor that distinguishes different types of stepping motors from an electrical point of view. From the electrical and control system perspective, variable reluctance motors are distant from the other types. Both permanent magnet and hybrid motors may be wound using either unipolar windings, bipolar windings or bifilar windings.

1.3.1 *Variable Reluctance Motor*

This type of stepper motor is probably the easiest to understand from structural point of view and probably the complicated one from the operation point of view. This type of motor consists of a soft iron multi-toothed rotor and a wound stator. Since it doesn't have any windings on the armature, rotor is easy to manufacture. When the stator windings are energized with DC current the poles become magnetized. Rotation occurs when the rotor teeth are attracted to the energized stator poles. Figure 1 shows a cross section of a typical V.R. stepper motor [9].

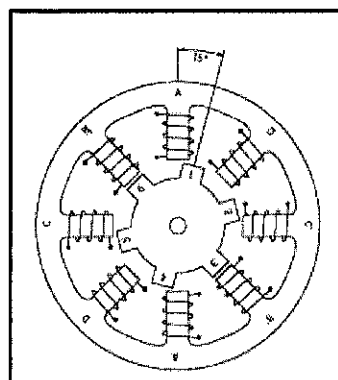


Figure 2: Cross section of a Variable Reluctance Motor [9]

In [3], authors have tried to do the structural modifications in the motor instead of proposing any controller. They had been successful in reducing the torque ripple, vibration as well as getting speed regulation to some extent. But the design proposed is quite difficult and make the motor more expensive. While in [4], author has attempted to adopt completely different approach by using the Phase current modulation. This technique is very simple and requires no modifications or digital calculations but it only covers the torque ripple minimization. Inductance versus angle variation of motor is assumed linear in the positive torque production period.

2.1.1 Techniques & Algorithms Applied

The advent of power electronics and fast digital hardware, together with improved nonlinear and adaptive control methods, enables a reevaluation of the issues related to switched reluctance motors. The objective is to reduce the nonlinearities and torque ripple by optimizing the motor performance. Through the literature, I came across different control techniques that have been applied to improve the motor performance. The motor indeed has pros and cons with itself. Some of the other techniques that have been applied are:

- Spline Function Modeling using adaptive rules
- Continuous sliding mode control technique
- Adaptive fuzzy logic controller using least-means-square algorithm

All of the above techniques have been applied to minimize the ripple to some extent, obtain speed regulation and improve the current profile of the motor. Thus In this project, I will try to improve the similar performance parameters by first modeling the motor in SIMULINK MATLAB and later applying some control strategies with particular controller.

energized coils, minimizing the flux path. The motor moves clockwise when winding 1 is turned off and winding 2 is energized. The rotor teeth marked Y are attracted to winding 2. This results in 30 degrees of clockwise motion as Y lines up with winding 2. Continuous clockwise motion is achieved by sequentially energizing and de-energizing windings around the stator.

The following control sequence will spin the motor depicted in Figure 4 clockwise for 12 steps or one revolution.

Winding 1: 1001001001001

Winding 2: 0100100100100

Winding 3: 0010010010010

The relationship among step angle, rotor teeth, and stator teeth is expressed using the following equation:

$$\theta = \left(\frac{N_s - N_r}{N_s N_r} \right) 360^\circ$$

where θ = step angle in degrees, N_s = Number of teeth on stator core and N_r = Number of teeth on rotor core

2.2.4 Energy Conversion Principles of Switched Reluctance Motor

The energy conversion principles of the switched reluctance motor are viewed in aspects of its magnetization curves which include the analysis of the 3 most important positions analyzed in SRM which are aligned position, unaligned position and intermediate rotor position. Instantaneous torque and average torque are also other two of the important aspects that should be understood.

Aligned Position

The aligned position as shown in figure 5 shows a pair of rotor, exactly in line with a pair of stator. During this position, there is no torque because rotor is at the position of maximum inductance. Maximum inductance phenomena happen because the magnetic reluctance of the flux path is at its lowest when the current flow. However when the rotor moves in either direction, it will produce a restoring torque that tries to maintain the position to achieve maximum inductance.

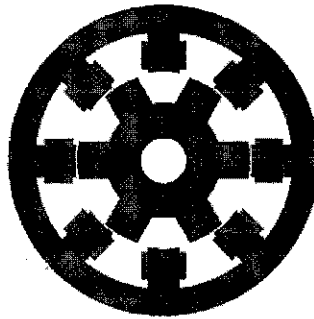


Figure 6: Aligned Position of SRM

Unaligned Position

The unaligned position is as shown in figure 6. The rotor poles are not in line with the stator poles and minimum phase inductance exists because magnetic reluctance of the flux path is at its highest. There is no torque during this position unless the rotor is moved in either direction, attracting it to the second phase being excited.

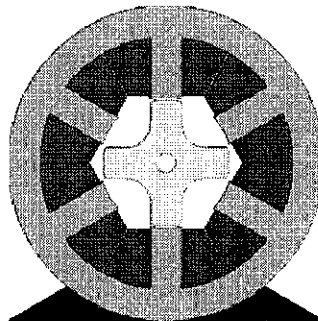


Figure 7: Unaligned Position of SRM

Intermediate Position

The position of rotor poles is between the position of aligned and unaligned.

To understand the relationship between number of teeth and the degrees of step, consider the Figure 7. In this circuit, the stator has six teeth and the rotor has four teeth. According to Equation mentioned, the rotor will turn 30° each time a pulse is applied. Figure 7 (a) shows the position of the rotor when phase A is energized. As long as phase A is energized, the rotor will be held stationary. When phase A is switched off and phase B is energized, the rotor will turn 30° until two poles of the rotor are aligned under the north and south poles established by phase B. The effect of turning off phase B and energizing phase C is shown in Figure 7 (c). In this circuit, the rotor has again moved 30° and is now aligned under the north and south poles created by phase C. After the rotor has been displaced by 60° from its starting point, the step sequence has completed one cycle.

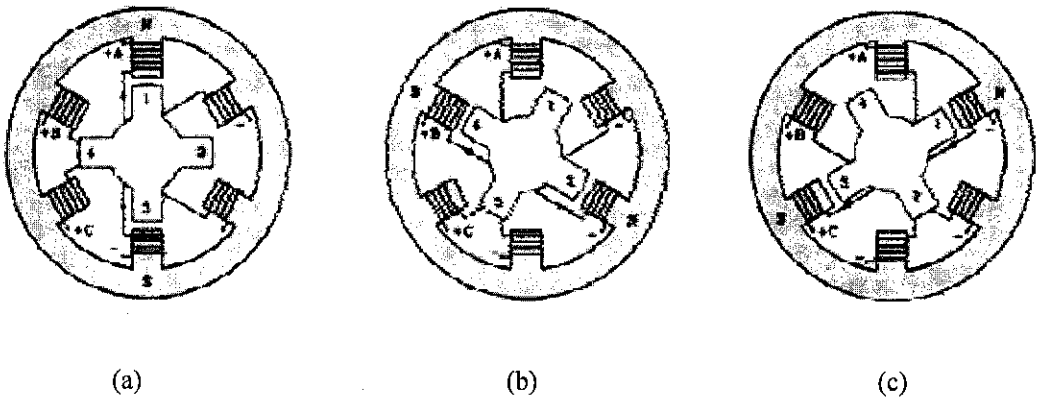


Figure 8: Rotor Switching Sequence of VRM

The Switching Sequence to complete a full 360 degrees of rotations for a variable reluctance motor with six stator poles and four rotor poles is shown in Table 1. By repeating this pattern, the motor will rotate in a clockwise direction. The direction of the motor is changed by reversing the pattern of turning ON and OFF each phase.

Table 1: Switching Sequence of the SRM

Cycle	Phase			Position
	A	B	C	
1	ON	OFF	OFF	0 degrees
	OFF	ON	OFF	30 degrees
	OFF	OFF	ON	60 degrees
2	ON	OFF	OFF	90 degrees
	OFF	ON	OFF	120 degrees
	OFF	OFF	ON	150 degrees
3	ON	OFF	OFF	180 degrees
	OFF	ON	OFF	210 degrees
	OFF	OFF	ON	240 degrees
4	ON	OFF	OFF	270 degrees
	OFF	ON	OFF	300 degrees
	OFF	OFF	ON	330 degrees
5	ON	OFF	OFF	330 degrees

2.2.5 Basic Control Circuit

Variable reluctance motors have multiple windings, typically three to five, which are all tied together at one end. The windings are turned on one at a time in a particular sequence to turn the motor. Figure 8 shows the basic circuit for driving a variable reluctance motor. Note the diodes across the windings.

As with all inductive loads, as voltage is switched on across a winding, the current in the winding begins ramping up. When the switching MOSFET for the winding is turned off a voltage spike is produced that can damage the transistor. The diode protects the MOSFET from the voltage spike assuming the diode is adequately sized [9].

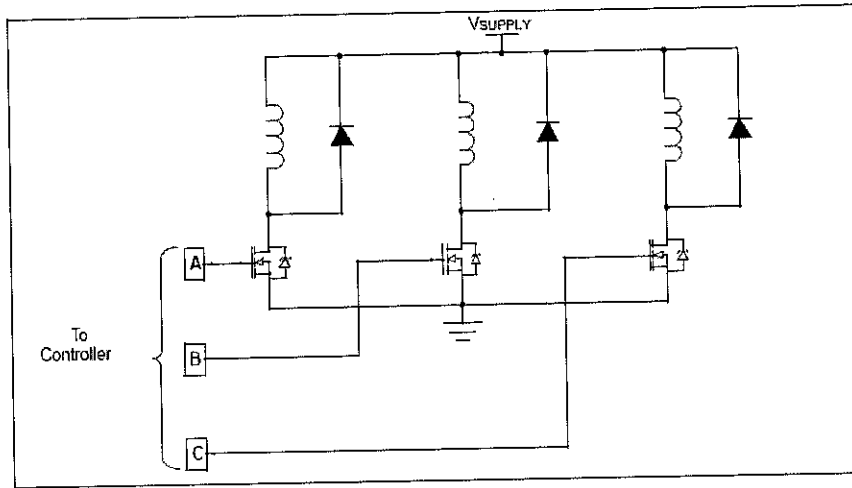


Figure 9: SRM Control Circuit

2.2.6 Torque- Speed Characteristics

The torque-speed operating point of a SRM is essentially programmable and determined almost entirely by the control. This is one of the features that make the SRM an attractive solution. The envelope of operating possibilities, of course, is limited by physical constraints such as the supply voltage and the allowable temperature rise of the motor under increasing load. In general, this envelope is described by Figure 9.

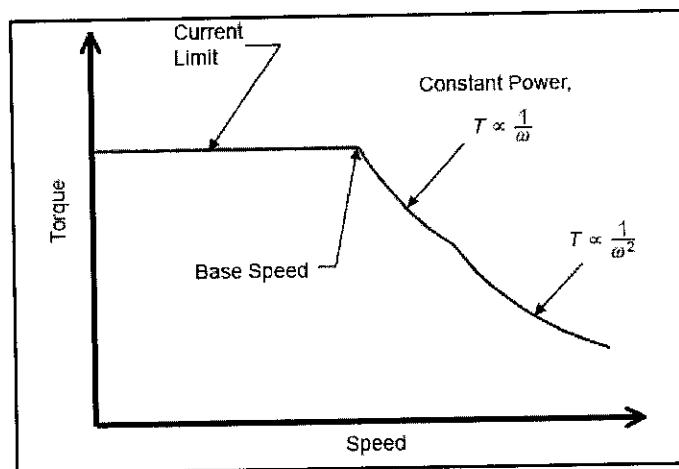


Figure 10: SRM torque speed characteristics [6]

Like other motors, torque is limited by maximum allowed current, and speed by the available bus voltage. With increasing shaft speed, a current limit region persists until the rotor reaches a speed where the back-EMF of the motor is such that, given the DC bus voltage limitation we can get no more current in the winding—thus no more torque from the motor. At this point, called the base speed, and beyond, the shaft output power remains constant, and at it's maximum. At still higher speeds, the back-EMF increases and the shaft output power begins to drop. This region is characterized by the product of torque and the square of speed remaining constant [6].

3.3 Insight into Switched Reluctance Motor

In order to control a SRM, it is very necessary to have some control using fast switching power converters. The one of the example used to control has been identified in the Basic Control Circuit part of Introduction.

Electromechanical energy conversion may be considered as consecutive transformation of electrical energy into magnetic energy and of magnetic energy into mechanical energy. The transformation of electrical energy into magnetic energy is described by the differential equation

$$\frac{d\psi_j}{dt} = v_j - Ri_j, j = 1, \dots, 4$$

The coenergy (W_j) of the magnetic field is obtained as an integral at constant rotor position θ , where magnetic energy does not convert into mechanical energy:

$$W_j(\theta, i_j) = \int_0^{i_j} \psi_j(\theta, i_j) di_j$$

Transformation of magnetic co-energy into mechanical energy without exchange between the winding and the electrical supply at constant current generates torque and is determined by differentiating the co-energy function W_j with respect to θ at constant current, i.e.,

$$T_j(\theta, i_j) = \frac{\partial W_j}{\partial \theta} \quad j = 1, \dots, 4$$

The torque generation can also be explained by the tendency of the magnetic circuit of the motor to a minimum configuration of reluctance, i.e. determining the rotor poles to move into alignment with the energized stator poles, while the inductance of the excited phase is maximized. Sustainable rotational motion is achieved by successively feeding the different phases, depending on the position of the rotor as the rotor turns. If the energized phase is not driven into saturation, the flux linkage be expressed as follows:

$$\psi_j(\theta, i_j) = L(\theta) i_j(\theta)$$

which is the product of phase current and the phase inductance. Thus, by using the above equations, the expression for torque can be derived and is given by

$$T_j(\theta, i_j) = \frac{1}{2} i_j^2 \frac{dL_j}{d\theta}$$

From above equation, it is immediately understood that the generated torque is independent of the direction of current flow. Hence, unidirectional currents are generally used, thereby, greatly simplifying the design of the power converter. A better understanding of the relationship between the phase inductance profile and the torque profile can be obtained from figure 10 where the top figure shows the inductance variations of one typical phase and the corresponding torque profile at constant current is shown in the bottom figure. The description of the various angular positions is explained below [13].

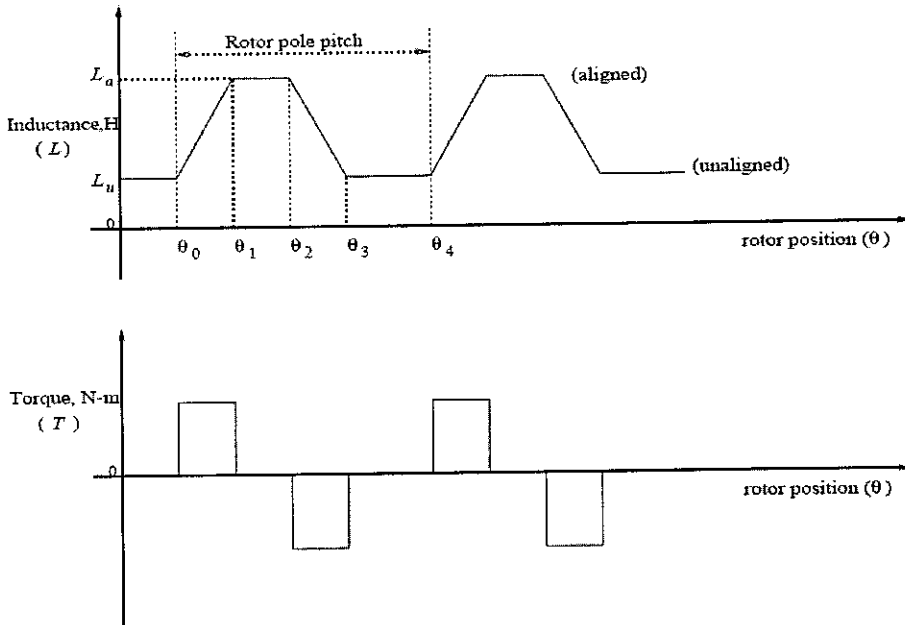


Figure 11: Variation of Inductance and Torque of one phase [10]

- At θ_0 , the leading edges of the rotor poles meet the edges of the stator poles and the inductance starts a linear increase with rotation, continuing until the poles are fully overlapped at θ_1 , when the inductance reaches its maximum value L_a . Ideally, $\theta_1 - \theta_0 = \beta_s$ (stator pole arc).
- From θ_1 to θ_2 , the inductance remains constant at L_a through the region of complete overlap. Ideally, $\theta_2 - \theta_1 = \beta_r$ (rotor pole arc).
- From θ_2 to θ_3 , the inductance decreases linearly to the minimum value L_u . Hence, $\theta_3 - \theta_2 = \beta_s + \beta_r$.
- From θ_3 to θ_4 , the stator and rotor poles are not overlapped and the inductance remains constant at L_u . So, the rotor pole pitch $\alpha_r = \theta_4 - \theta_3$.

From above figure and rotor position analysis, we can conclude to following results.

- If $\frac{dL}{d\theta} < 0$, then $T > 0$. It is a case of motoring torque production.
- If $\frac{dL}{d\theta} > 0$, then $T < 0$. It is a case of generating torque production.

It is clear that for the motor to be able to start in one direction (forward) from any initial rotor position, the pole arcs must be chosen such that at least one of the phase windings is in a region of increasing inductance (or decreasing inductance for rotation in the reverse direction). Further, in order to produce a unidirectional forward motoring torque, the stator phase windings have to be sequentially energized such that the current pulse for a phase must coincide with the angular interval where the $\frac{dL}{d\theta}$ for that phase is positive. Similarly, a braking torque (generating mode) or reverse rotation (motoring in the reverse direction) is obtained when the current

pulses coincide with the angular intervals where the respective $\frac{dL}{d\theta}$ is negative.

Therefore, a rotor position sensor is obviously required to start and stop the conduction of various phases. When this motor is operated without feedback control and the phase currents are switched on and off in sequence, the rotor will advance in steps of angle (called as Step angle) ϕ . For a three-phase SR motor with four rotor poles, $\phi = 30^\circ$.

Assuming that rotor pole arcs β_r is equal to stator pole arcs β_s , the relation between angles can be obtained as follows:

$$\theta_x = \left(\frac{\pi}{N_r} - \beta_r \right)$$

$$\theta_y = \frac{\pi}{N_r}$$

All the values of the parameters for designing a motor in SIMULINK are given in following table and all the initializations are given in Appendix II

Table 2: Important parameter values for design of SRM

PARAMETER	SYMBOL	VALUE
Moment of Inertia	J	0.0013
Viscous Friction Coefficient	B	0.0183
Resistance of Motor Phases	R	1.3 ohms
Number of Stator Poles	N_s	6
Number of Rotor Poles	N_r	4
Terminal voltage	V_n	150 V
Rotor pole arc	β_r	30°
Stator pole Arc	β_s	30°
Phase inductance at aligned positio	L_a	60mH
Phase inductance at un-aligned position	L_u	8mH

In terms of the Faraday's law, the flux-linkage ψ and voltage V_s for one phase during fluxing process can be expressed with:

$$\psi = \frac{1}{\omega} \int (V_s - Ri) d\theta$$

$$V_s = Ri + L(\theta, i) \frac{di}{d\theta} + \omega i \frac{dL(\theta, i)}{d\theta}$$

Where R represents the phase resistance, which increases with the rotor speed; $L(\theta, i)$ indicates the instant inductance value. In second equation above, the three terms on the right hand side represent the resistive, inductive and back EMF terms, respectively. If the phase resistance R is small, the flux-linkage will increase linearly with the rotor position. In terms of the inductance profile due to constant inductance around the unaligned position, the current increases linearly at first. However, when the rotor pole overlaps with the stator pole, the inductance increases with the rotor position θ and the back EMF starts to build up. As a result, the current rising rate is decreased. When the back EMF is larger than the input voltage V_s , the current starts to decrease. During “de-fluxing” period, the supply voltage reverses and the phase current drops to zero very quickly.

Torque Equation is given by:

$$T_e = \frac{1}{2} i^2 \frac{dL(\theta, i)}{d\theta}$$

In terms of the above equation it is obvious that the torque produced in the SRM depends on the phase current and rotor position. When the rotor is around the unaligned or aligned position, no torque is produced. If the phase current is constant, the torque is constant during the rotor is in the overlapped or intermediate position. Furthermore, positive torque is produced when the phase winding is excited during the rising inductance, and negative torque is produced during the falling inductance. Because the torque changes with the rotor position and current, although the current

flows to phase windings continually from the power supply, there is still a dip in the torque waveform at the commutation instant from one phase to the next one. There are two reasons for this. One is that each phase current always starts from zero; another one is that the change of the inductance with rotor position is small at the commutation instant. Thus Torque ripple is the major disadvantage of the SRM

3.3.1 SRM Energizing Strategies

There are several possible configurations to energize an SRM from a converter. The different energizing structures distinguish themselves by their number of semiconductors and passive components. They also depend on the number of phases and the way the stator coils are connected. Some of the famous energizing strategies are:

- Voltage Control Single Pulse Technique
- Current Control with Hysteresis Technique
- PI Control

3.3.2 Two quadrant Chopping Convertor

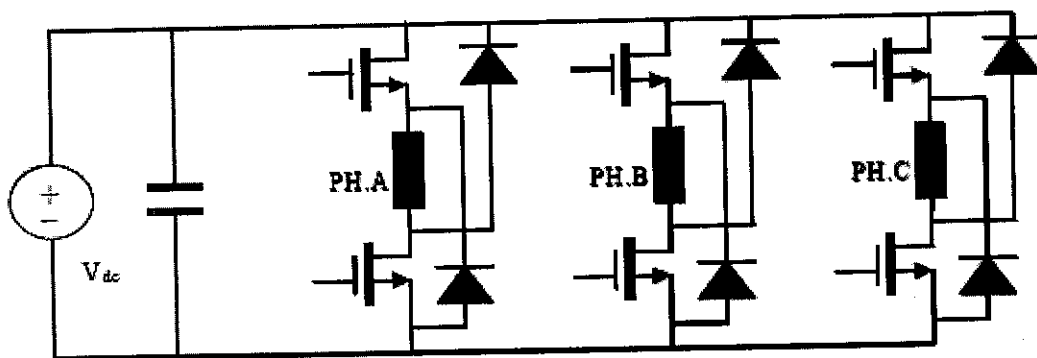


Figure 12: Two quadrant Chopping Convertor

Figure 11 shows the Two-Quadrant-chopping converter for the SRM. As mentioned before, in order to increase the reliability and realize certain control strategies, more than one switch per leg is used. This converter is similar to the conventional dc- ac converter, except that the motor winding is in series with the phase switches. Also,

the switches have voltage and current ratings that are similar to those of an equivalent AC converter drive.

This converter provides highest efficiency, reliability and control flexibility. The upper and lower switches can be controlled independently to realize different control schemes. For example, when the upper and lower switches are switched simultaneously, the two diodes on each leg provide the freewheeling path for “de-fluxing”. This control scheme is called hard chopping with which the negative voltage V_{dc} is provided during the “de-fluxing” process. If the lower switch conducts all the time, only the upper switch is switched, then the zero voltage is provided during the “de-fluxing” process, which is called the soft chopping. When the upper switch is turned off, the upper switch and the upper diode provides the freewheeling path for “de-fluxing”.

In addition, this converter can provide maximum regenerative braking capability and equal performance in forward and reverse directions. Also, there is no protection circuit needed to prevent shoot-through faults because the switches on each phase conduct simultaneously. All these advantages make the Two-Quadrant-chopping converter popular in SRM application.

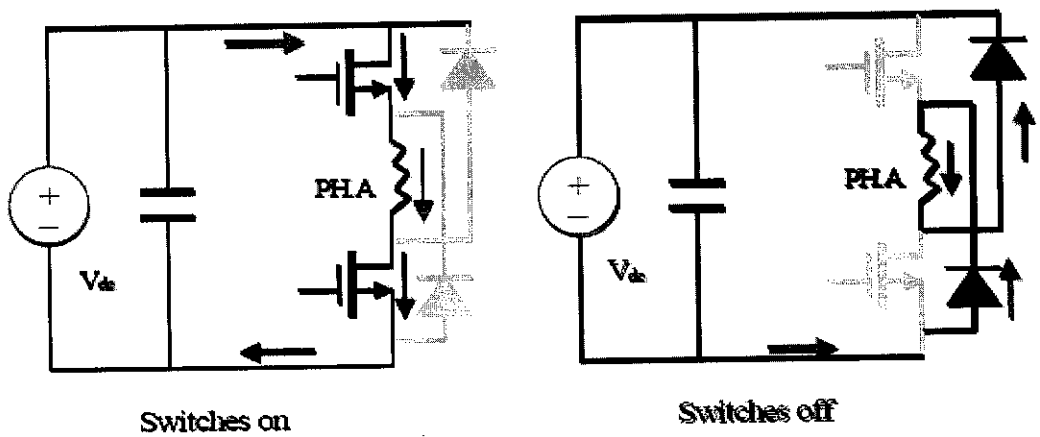


Figure 13: Switching of the Two quadrant Chopping Converter

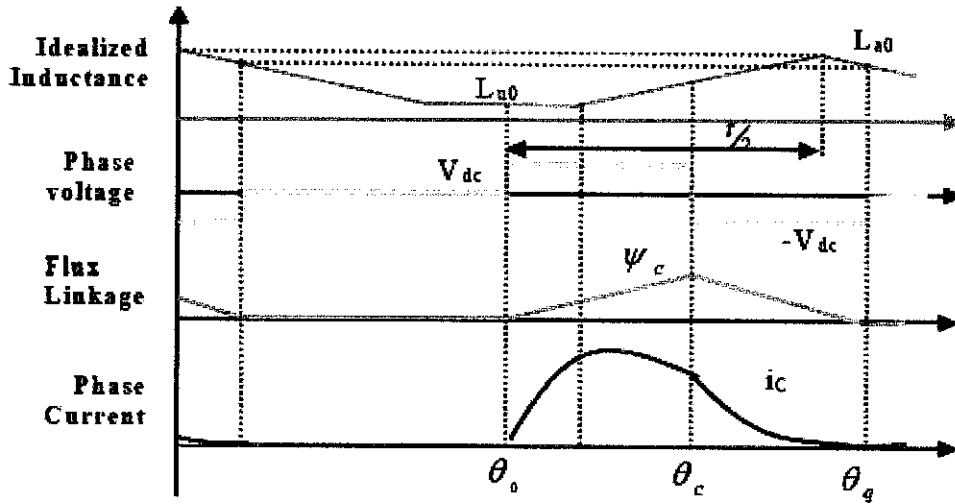


Figure 14: Results produced as a result of two quadrants Chopping Converter

3.3.3 Selection of Stator and Rotor Pole arcs

When the rotor pole arc is greater than that of the stator pole arc then there is no benefit in terms of torque production if ideal current turn-off (i.e. zero time for current to go from an operating value) is assumed. But in practical SRM, ideal current turn off is impossible as they have inductances to cater for. Thus it becomes necessary to turn off the currents even before they reach the completely aligned position. Hence to utilize the torque-producing positive inductance slope region completely, it is important that the current be maintained in the region. If the current continues beyond the positive slope region, then a negative torque is produced since with equal pole arcs, there is no zero slope inductance regions.

In order to best utilize the positive slope of inductance for torque production, the current fall angle is calculated and is used to know the turnoff angle exactly. But it should be clear that, when advanced turnoff is achieved, the average torque is reduced. Thus considering all this, some of the practical motors are designed with rotor arc greater than that of stator pole arc.

Following observations are achieved with this configuration.

- Negative torque generation can be avoided entirely with a dead zone given by $\beta_r - \beta_s$, where no torque is produced even when there is current, thus increasing the average torque contribution of a phase.
- Precise calculation of current call angles is not required for every operating condition.
- Elimination of negative torque generation reduced the torque ripples and hence the audible noise generation. The increase in the average torque as well as other advantages in both steady state and transient operating conditions is achieved.

3.3.4 Summary of SRM Modeling Equations

The mechanical part of the motor equations is derived using Newton's law, which states that the inertial load J times the derivative of angular rate equals the sum of all the torques about the motor shaft. The result is this equation which is the relation between the electrical and mechanical parts of SR motor; it can be stated as:

$$J \frac{d\omega}{dt} = \sum \tau_i$$

$$J \frac{d\omega}{dt} = T(i, \theta) - T_L - B\omega$$

$$\frac{d\omega}{dt} = \frac{1}{J} (T(i, \theta) - T_L - B\omega) \dots\dots\dots (1)$$

where T_L is the Load Torque, $T(i, \theta)$ is the generated phase torque (motor torque), θ is the angular position of the rotor, J is the moment of inertia and B is the viscous friction coefficient.

The **instantaneous voltage** across the terminals of a single phase of an SR motor winding is related to the flux linked in the winding by Faraday's law,

$$V_n = RI_n + \frac{d\phi_n}{dt} \quad (n=1,2,3\dots)$$

$$\frac{d\phi_n}{dt} = -RI_n + V_n \dots\dots\dots(2)$$

where V_n is the terminal voltage, I_n is the phase current, R is the phase resistance and ϕ_n is the flux linkage of the Phase

Angular Velocity of Motor $\omega = \frac{d\theta}{dt} \dots\dots\dots(3)$

Instantaneous Torque of phase

$$T_n = \frac{d}{d\theta} (W'(\theta, i)) \quad (n=1,2,3,\dots)$$

$$T_n = \frac{d}{d\theta} \int \phi_n(\theta, i_n) di$$

$$T_n = \frac{1}{2} i_n^2 \frac{dL_n(\theta)}{d\theta} \dots\dots\dots(4)$$

where $W'(\theta, i)$ is the magnetic field co-energy and L_n is the phase inductance of nth phase.

The Equation (4) suggests that positive (or motoring) torque is produced when the motor inductance is rising as the shaft angle is increasing $\frac{dL}{d\theta} > 0$. Thus, the desired operation is to have current in the SRM winding during this period of time. Similarly, a negative (or braking) torque is produced by supplying the SRM winding with current while $\frac{dL}{d\theta} < 0$

Torque Ripple of phase

$$TR = \frac{T_{instMax} - T_{instMin}}{T_{avg}} \dots\dots\dots(5)$$

Average Torque

$$T_{avg} = 1/T \int_0^T T_{inst} .dt \dots\dots\dots(6)$$

Operating Thetas

$$\theta_1 = \frac{\pi}{Nr} - \left(\frac{\beta r + \beta s}{2} \right)$$

$$\theta_2 = \theta_1 + \beta s$$

$$\theta_3 = \theta_2 + (\beta r - \beta s)$$

$$\theta_4 = \theta_3 + \beta s$$

$$\theta_5 = \theta_4 + \theta_1 = \frac{2\pi}{Nr}$$

3.3.5 Application Example

Before the SRM is simulated in MATLAB/SIMULINK with all the design parameters, the author managed to obtain an application example which was simulated using the SRM model available in SIMULINK library. By using this example, better understanding of the controller's operation and motor performance is obtained.

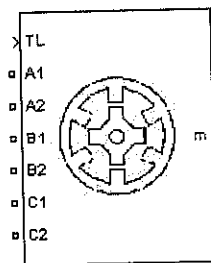


Figure 15: Model of SRM available in MATLAB

Configurations available for Simulations

The Switched Reluctance Motor (SRM) block represents three most common switched reluctance motors: three-phase 6/4 SRM, four-phase 8/6 SRM as well as five-phase 10/8 SRM. For simulation purpose two models can be selected, a generic model or a specific model. The **generic model** is characterized by the aligned and unaligned inductances, the saturated aligned inductance, the maximum current and the maximum flux linkage, while the **specific model** is characterized by the magnetization characteristics given as a table of flux linkage in function of the rotor position and the stator current.

Inputs and Outputs

TL: The block input is the mechanical load torque (in N.m). TL is positive in motor operation and negative in generator operation.

m: The block output ‘m’ is a vector containing several signals. We may demultiplex these signals by using the Bus Selector block from Simulink library.

Table 3: Signals to be selected as an output

Signal	Definition	Units
V	Stator voltages	V
Flux	Flux linkage	V.s
I	Stator currents	A
Te	Electromagnetic torque	N.m
W	Rotor speed	rad/s
Teta	Rotor position	rad

Converter Used

The SRM is fed by a three-phase power converter having three bridge converters, each of which consists of two IGBTs and two free-wheeling diodes as shown in Figure. During conduction periods, the active IGBTs apply positive source voltage to the stator windings to drive positive currents into the phase windings. During free-wheeling periods, negative voltage is applied to the windings and the stored energy is returned to the power DC source through the diodes. The fall time of the currents in motor windings can be thus reduced.

To develop positive torque, the currents in the phases of a SRM must be synchronized to the rotor position. Turn-on and turn-off angles refer to the rotor position where the converter's power switch is turned on and turned off, respectively. By using a position sensor attached to the rotor, the turn-on and turn-off angles of the motor phases can be accurately imposed. These switching angles can be used to control the developed torque waveforms.

Simulation of SRM drive

The example available in the library is run and simulated in order to have a view on the Motor output parameters. Three phase 6/4 SRM is chosen in the example considering the simplicity of the controller. A DC supply voltage of 240 V is used. The converter turn-on and turn-off angles are kept constant at 45 deg and 75 deg, respectively, over the speed-range.

The SRM is started by applying the step reference to the regulator input. The acceleration rate depends on the load characteristics. Since only the currents are controlled, the motor speed will increase according to the mechanical dynamics of the system. The SRM drive waveforms (phase voltages, magnetic flux, windings currents, motor torque, and motor speed) are displayed on the scope.

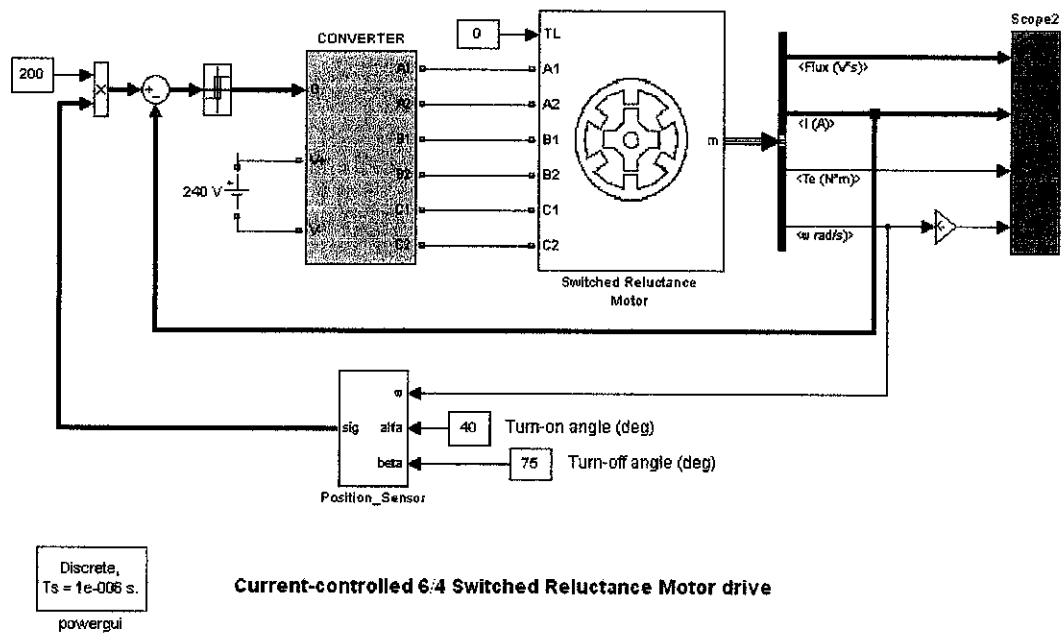


Figure 16: MATLAB blocks for the SRM simulation

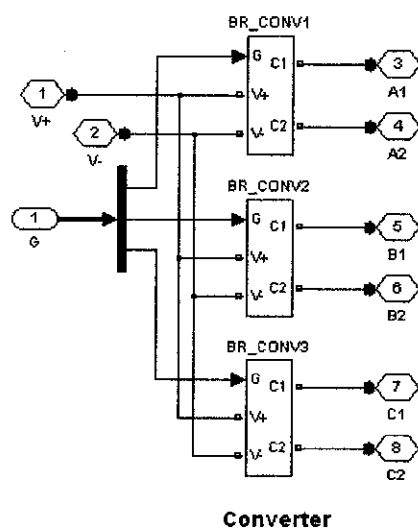


Figure 17: Converter Block

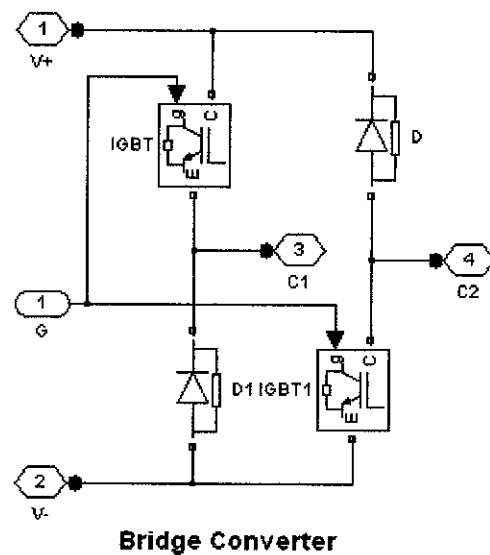


Figure 18: Sub-Converter Block

Output of the Simulation

The simulation results are observed at the Scope of the Motor, where in we have selected the output of Flux Linkage, Phase Current, Electrical Torque and the Speed. The four parameters are compared with each other for the time of simulations.

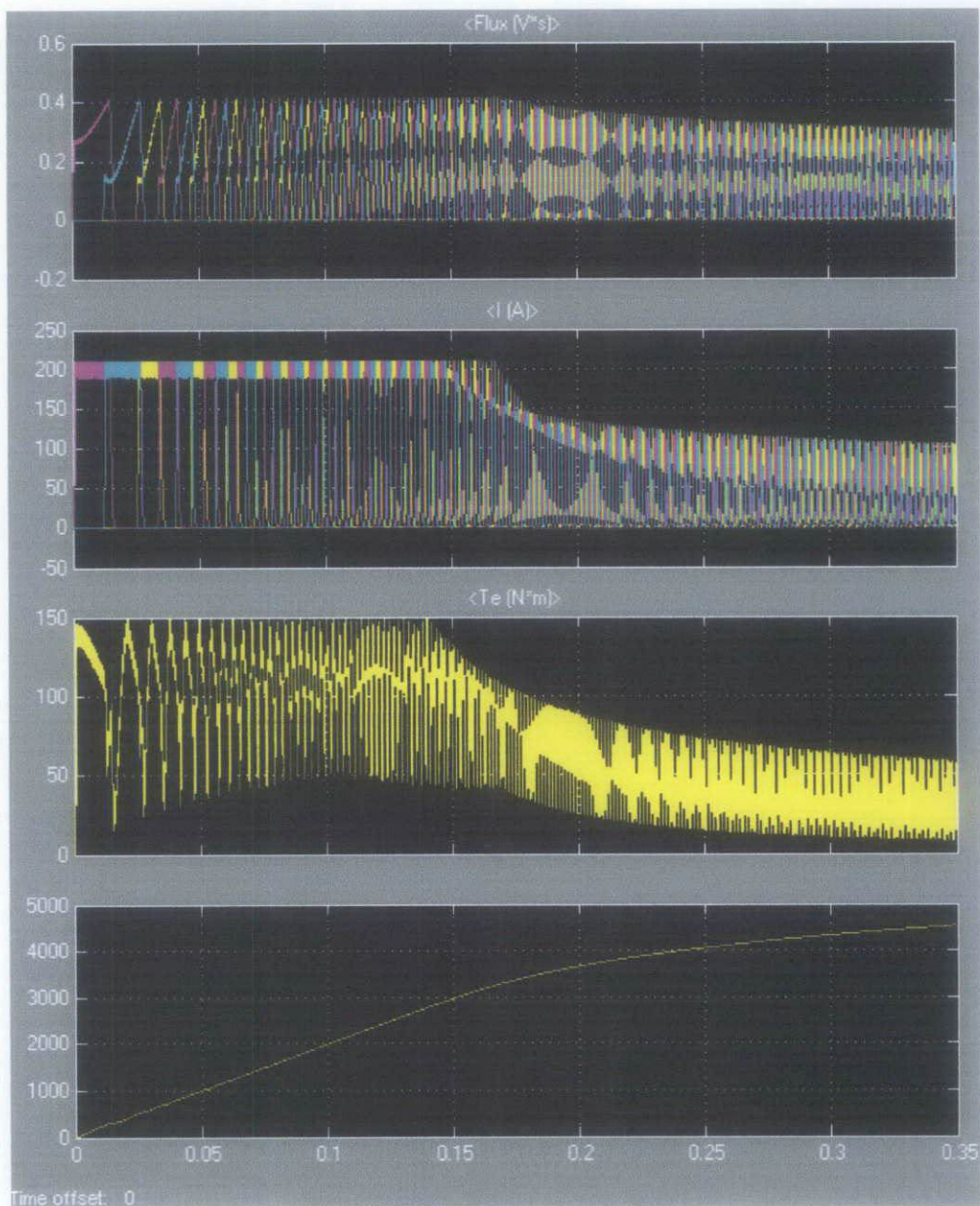


Figure 19: Output of the SRM

Output at Low Speeds

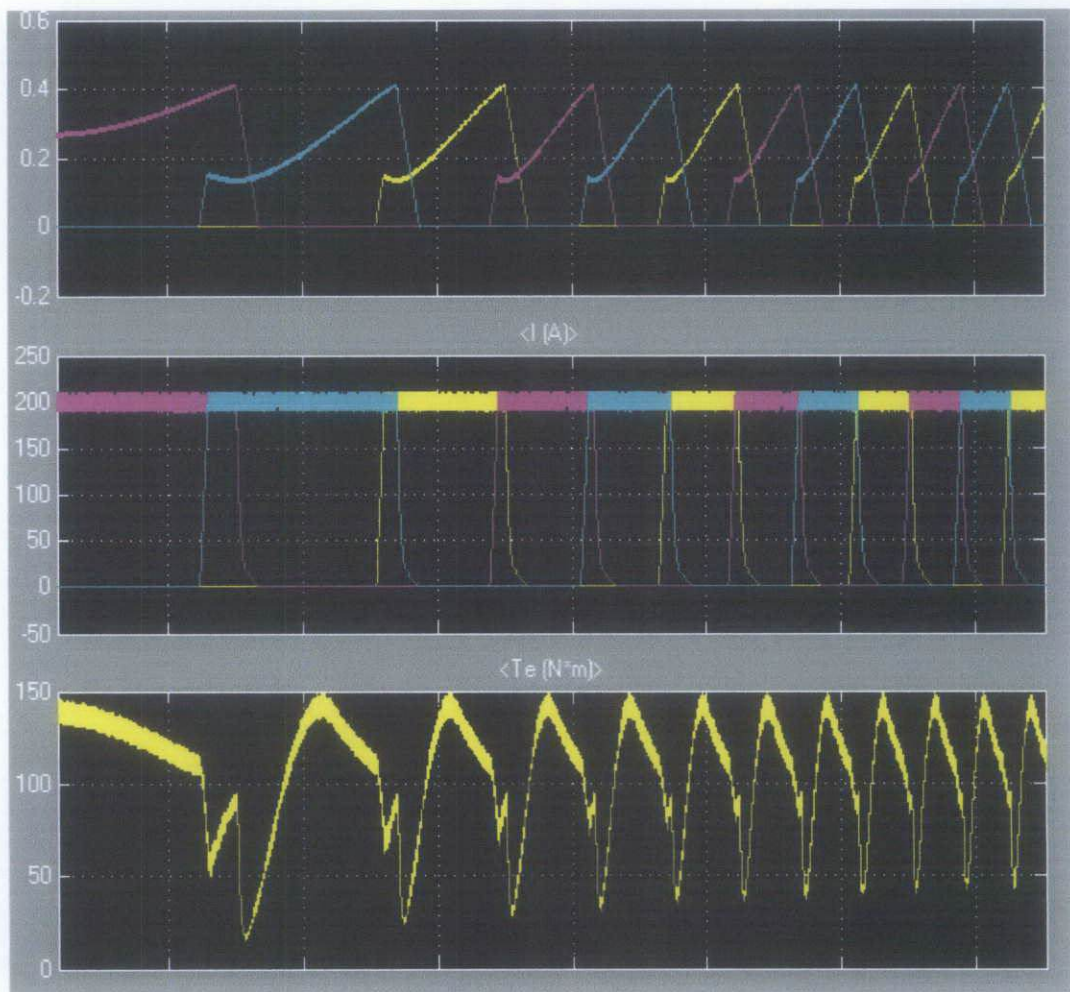


Figure 20: Output of the SRM at low speeds

After simulating the application example, we are aware of the performance parameters as well as output expected with them. The simulation helped a lot in understanding the working of Converter. The Simulations show, that there is a lot of torque ripple experienced because of the transitions of the supply to phases. Hysteresis Control technique is implemented for lower speeds and for higher speeds voltage pulse control is used. After this simulation, we will try to implement the SRM having similar results to these.

CHAPTER 4

RESULTS & DISCUSSIONS

In this project, an attempt is made to do the performance analysis of two configurations of the motor, i.e. motor with three phases 6/4 and motor with four phases 8/6. The purpose of analyzing two motor's configurations is to understand the complexity involved in simulating the two motors as well as differentiating them on the basis of outputs like Total Torque and Produced Speed.

For each kind of motor, simulation is done using two control techniques i.e. Voltage control and Current Control and the results are recorded and analyzed. Load analysis is also performed on each kind of motor with each control technique applied, where in maximum load and nominal loads are calculated for each strategy.

Initially in order to model the Motor, its dynamic equations have to be modeled in SIMULINK. The motor's torque equation given in (1) is modeled with following block configurations.

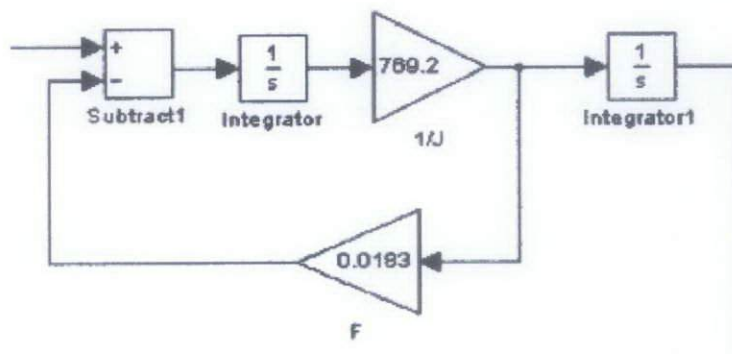


Figure 21: Mechanical equation block diagram via SIMULINK

4.1 Simulation of 6/4 SRM

This motor has three phases and six stator poles, while four rotor poles. Each phase of the motor is independent from other and is similar to other with only the phase shift of 30 degrees. Each phase of the motor needs to be energized at least once in order to move the rotor by 90 degrees, thus in order to complete one revolution of the motor, each phase has to be energized 4 times. ($90 \times 4 = 360$). The complete simulation of the 6/4 SRM is given in following figure.

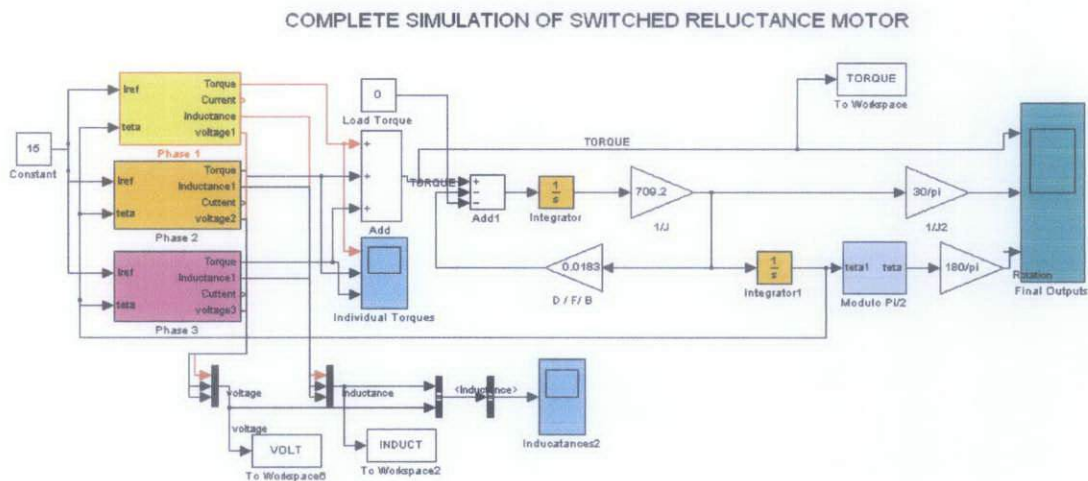


Figure 22: Complete Simulation Model of SRM

Each phase is fed back with the input of Position of the rotor, usually measured with the sensor attached to the motor and the reference current that is used for the hysteresis purposes. Using the position as input, each phase behaves accordingly, producing its output of torque. All the individual torques from each phase are added together and then using the block configuration of **FIGURE 21**, the output of total torque, speed and position is measured and displayed using scope. Further the outputs like phase current, phase inductance, phase flux as well as phase voltages are calculated and obtained using Scope in SIMULINK.

The following figure gives further insight of each phase of SRM; since all the phases are alike, only one phase (phase A) is shown here.

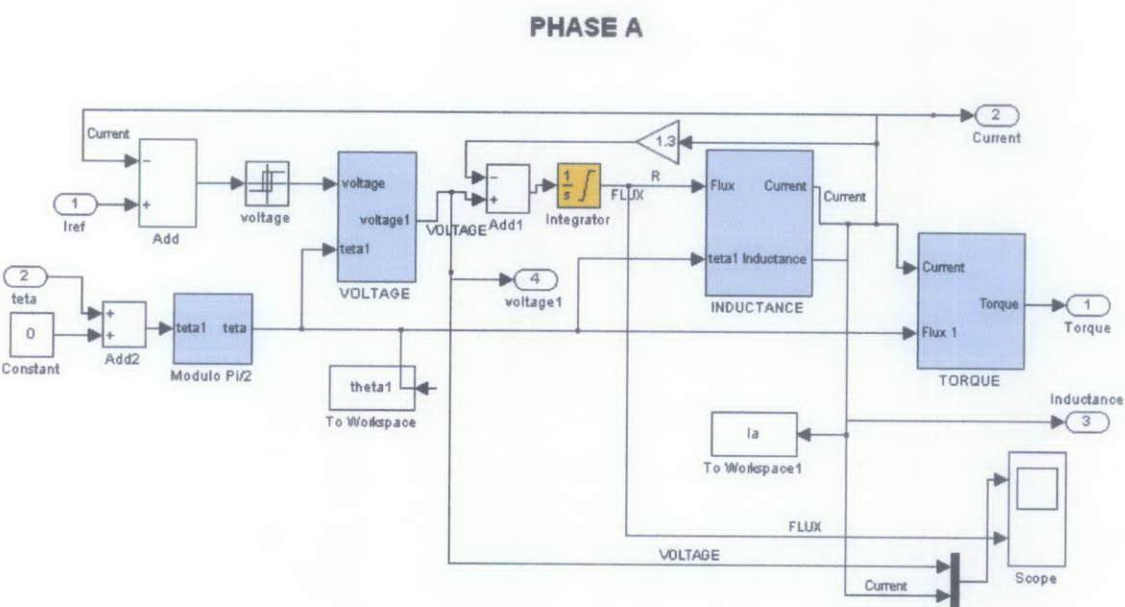


Figure 23: Phase Model of SRM

In above figure, equation (2) is simulated using the sub-block VOLTAGE, while equation (4) is simulated using the sub-block of TORQUE. Similarly the sub-block of INDUCTANCE is used to simulate the equation of inductance. The inputs are the position of the rotor and the reference current, while the outputs of current, flux and voltage are viewed through scope. Thus in order to simulate different equations and models, sub-block approach is used for clarification and better understanding. Different sub-blocks used in above figure are further explained and illustrated below:

Modulo pi/2: Each phase inductance has a periodicity of $\frac{2\pi}{N_r}$ degrees. Therefore, it is appropriate to transform the rotor position angle coming from the mechanical equation so that it is modulo $\frac{2\pi}{N_r}$. In figure below, block *modulo pi=2* achieves this

function. In the figure 24 phase shift of phase B is illustrated; the phase is 30 degrees displaced from the phase A.

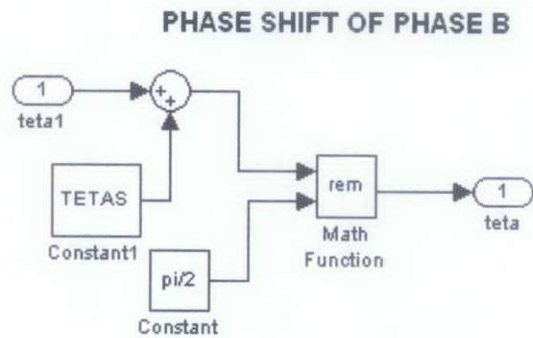


Figure 24: Modulo pi/2 Model

Voltage Sub-Block: *Voltage sub-block* is one of the most important sub-blocks for the SRM phase simulation. With the help of this sub-block, the Power converter discussed in the methodology is implemented using the blocks available in SIMULINK library such as if else block. Voltage sub-block permits to assure the power converter commutations at angles θ_{on} , θ_{off} , and θ_d , it is to assure the applications of single pulse operation is maintained.

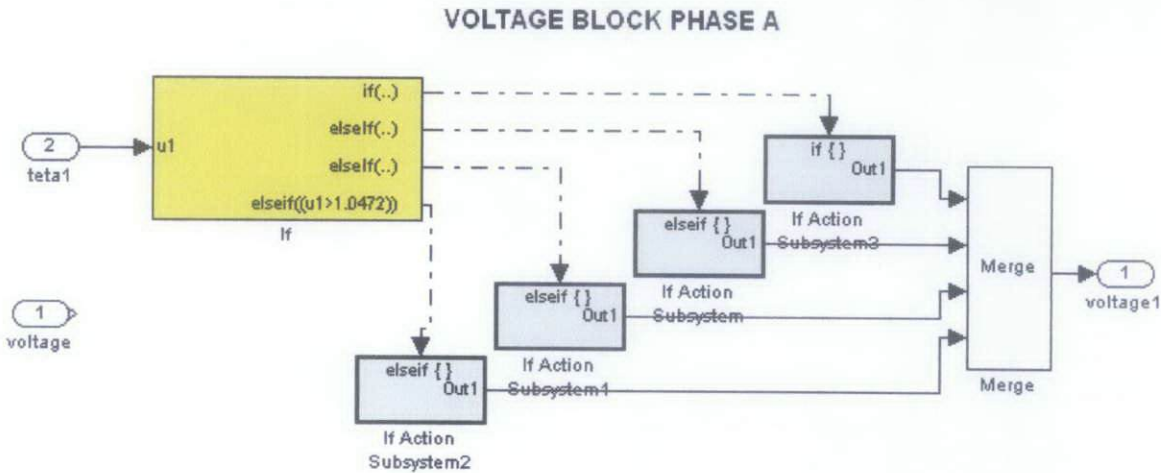


Figure 25: Voltage Model

Inductance Sub-Block: This *sub-block* computes the current and phase inductance according to rotor position θ and phase flux ψ . Therefore, one gets phase current I as its output signal, which is used for the calculation of Phase Torque, the block is shown in **FIGURE 26**

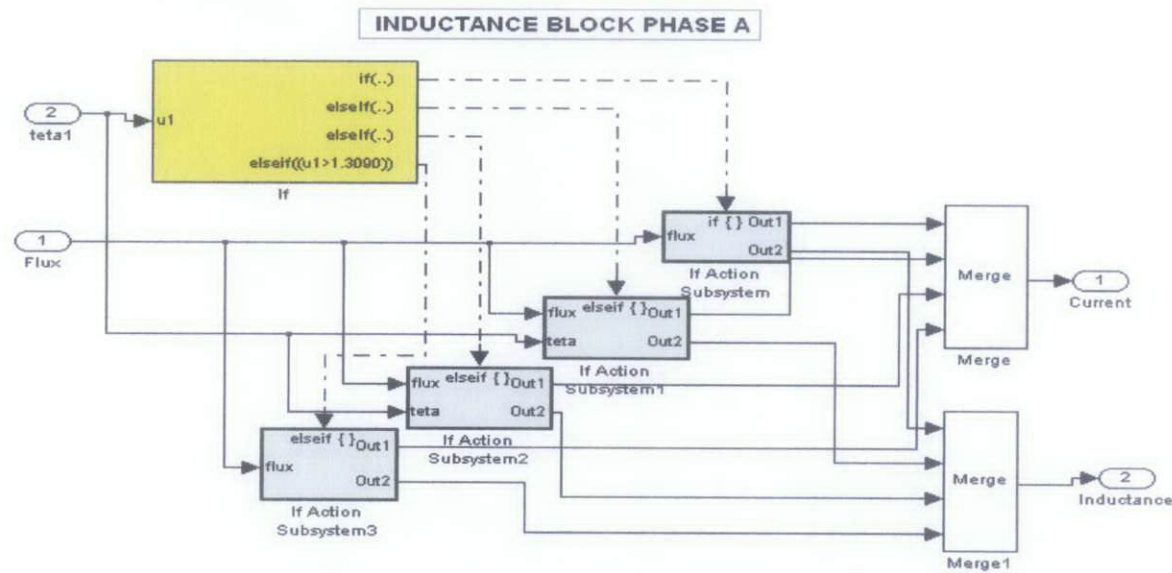


Figure 26: Inductance Model

The inductance sub-block produces the output of Inductance and current. The inductance produced keeps on varying depending on the position of rotor. It increases from the minimum inductance of L_u at unaligned position to maximum of inductance L_a at aligned position, which can be further understood from the chapter 3 discussed above The calculation of the various switching thetas is repeated here:

$$\begin{aligned} \theta_1 &= \frac{\pi}{Nr} - \left(\frac{\beta r + \beta s}{2} \right) \\ \theta_2 &= \theta_1 + \beta s \\ \theta_3 &= \theta_2 + (\beta r - \beta s) \\ \theta_4 &= \theta_3 + \beta s \qquad \dots\dots\dots(A) \\ \theta_5 &= \theta_4 + \theta_1 = \frac{2\pi}{Nr} \end{aligned}$$

Torque Sub-Block: It is used to compute the torque produced in each phase according to the rotor position θ and the current I . This block helps to implement the equation (4), where in it produces positive torque if the phase is supplied with current during positive slope of inductance, where as it produces negative torque if the phase is supplied with current during negative slope of inductance.

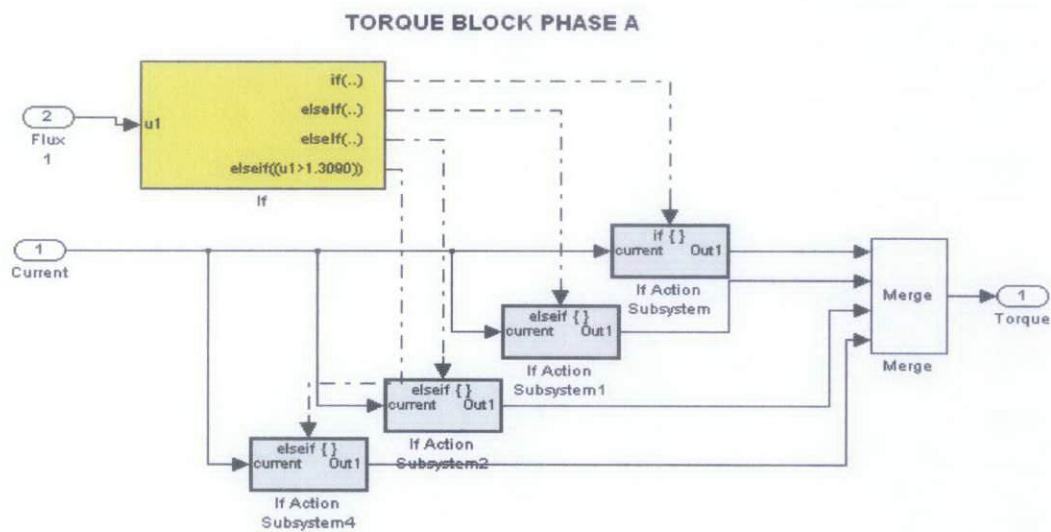


Figure 27: Torque Model

In order to analyze the performance of 6/4 SRM, different control strategies have been implemented and results are calculated in order to have complete insight of the motor. The summary of the different strategies applied for 6/4 SRM are given in following figure:

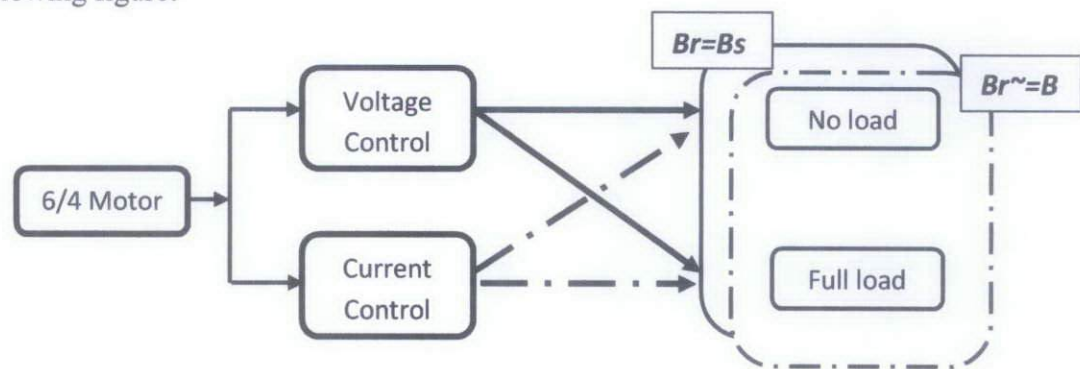


Figure 28: Summary of the different configurations implemented on 6/4 SRM

Thus firstly, we will apply the voltage control technique on 6/4 motor and analyze the performance with no load and variable load, after that we will change the stator arc/rotor arc ratio and then simulate again to find any improvements in the results. After that we will follow the same procedure for the Current Control Technique. Throughout the experiment, the motor is simulated with different set of θ on, θ off, and θ d. The theta value that produces negative torque will be discarded and hence will not be considered for any further calculations. In this way through trial and error, we will manage to select the best values of θ on, θ off, and θ d.

4.1.1 Simulation of 6/4 motor with Single Pulse Voltage technique with NO LOAD

Initially we choose $\theta_{on} = 20$ and $\theta_{off} = 30$ and we keep rotor and stator arcs equal i.e. $\beta_r = \beta_s = 30^\circ$. The values of θ_{on} and θ_{off} are chosen randomly to check the performance of motor. It should be kept in mind that since the Aligned Inductance is at $\theta = 45^\circ$ hence we will always keep the θ_{off} less than that value in order for current to reduce to zero before inductance starts to decrease again and produces negative torque.

Following graphs are obtained with the simulation of the motor when No Load is applied.

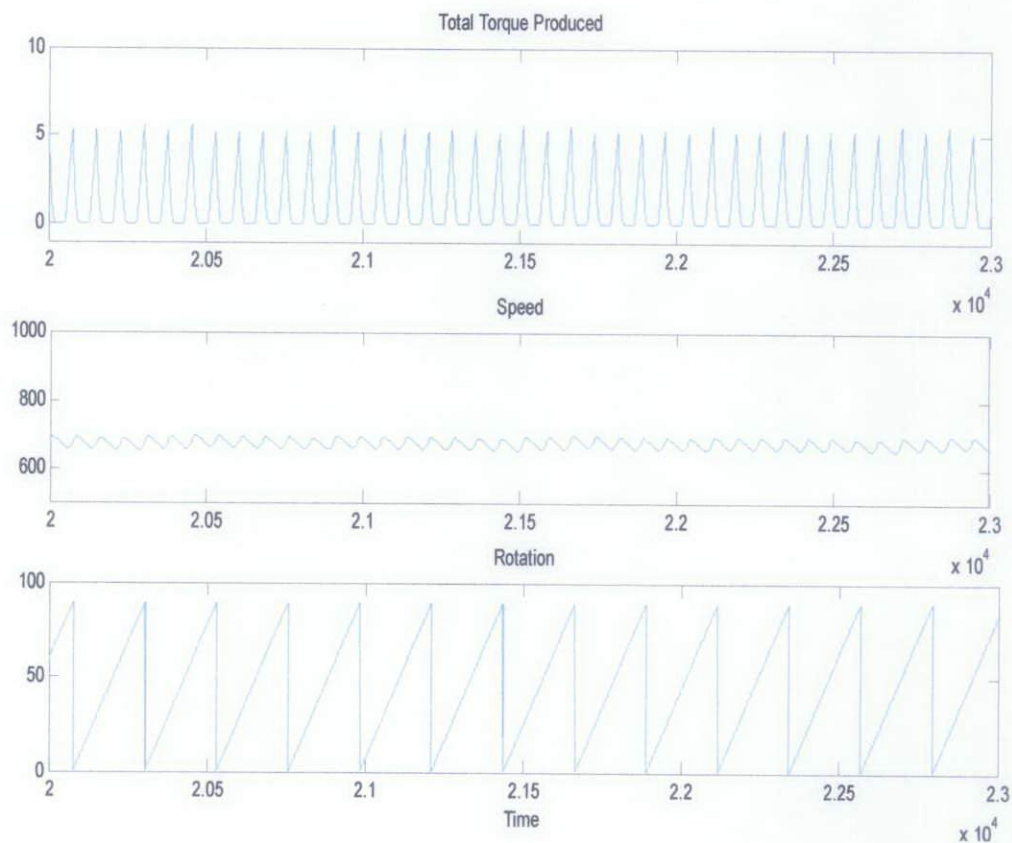


Figure 29: Output of Total Torque, Speed and rotation of 6/4 Motor at No load

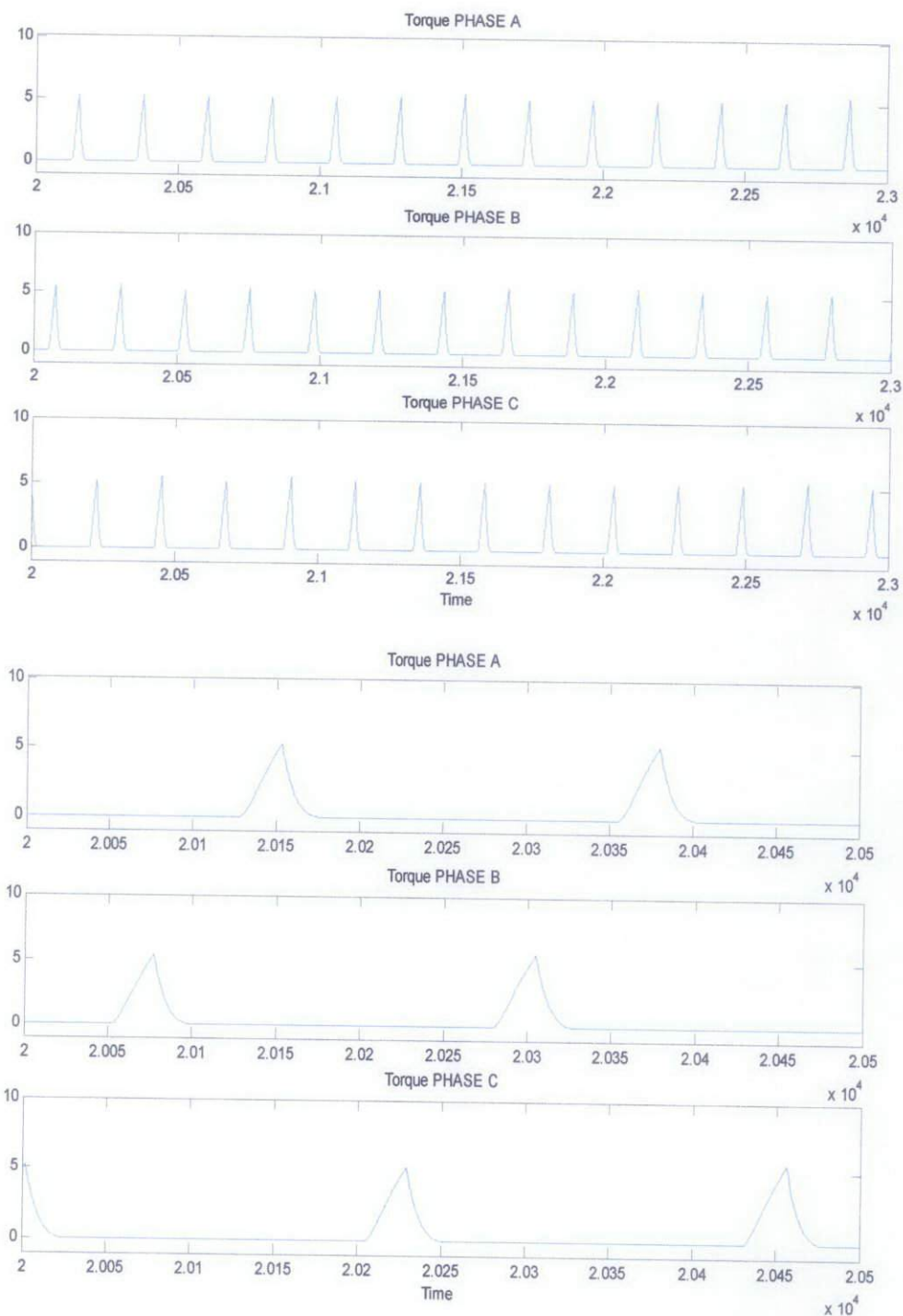


Figure 30: (a) Individual Torques generated from each phase, (b) Expanded view of Individual Torques generated

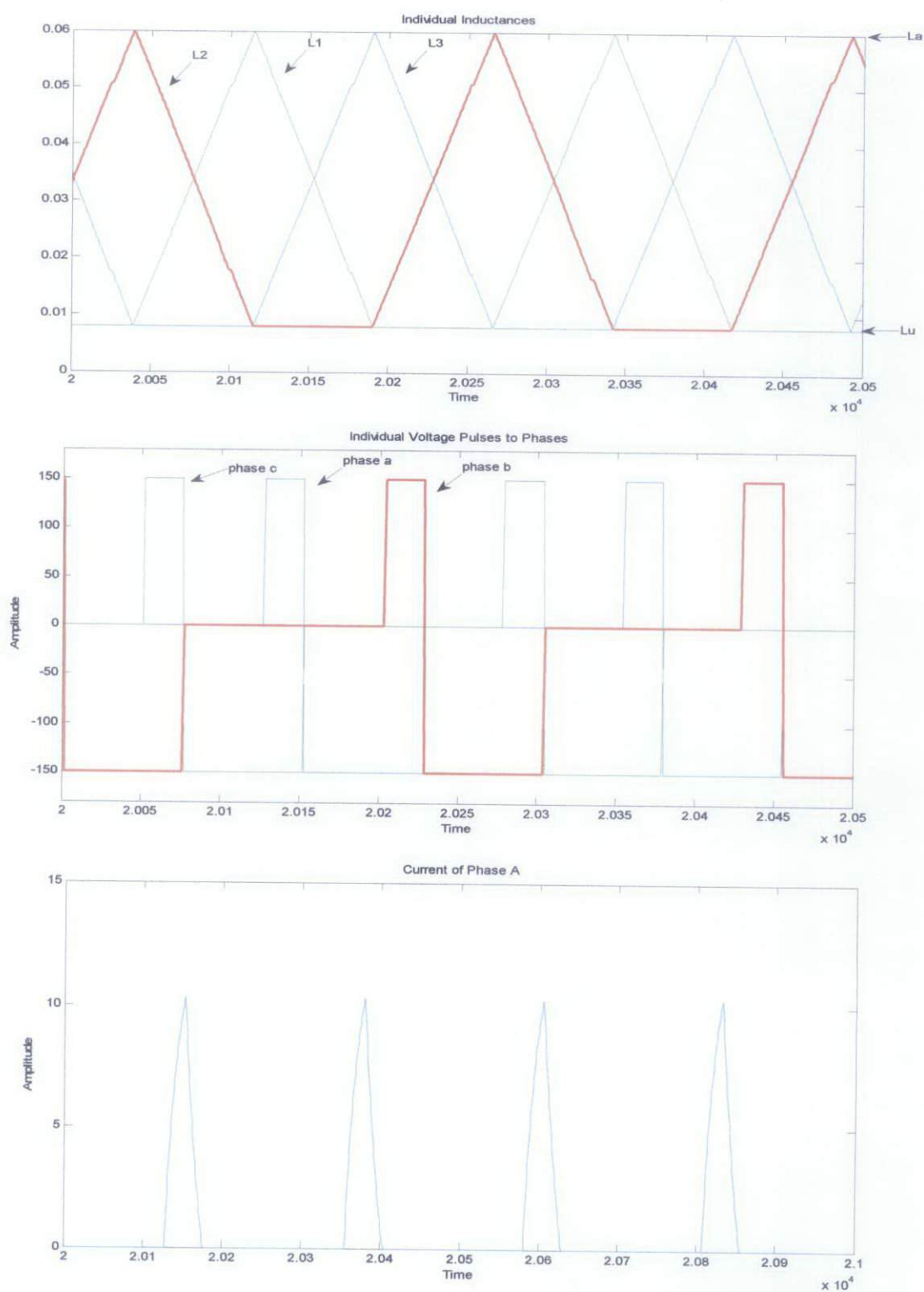


Figure 31: (a) Inductance profile of all the three phases, (b) voltage Pulses applied to three phases, (c) Current output of Phase A.

Interpretation of Graphs

In figure 29, it is demonstrated that Maximum torque of 5 N.m and Mean torque of 1.2767 N.m is produced with No load. In ideal case there should not be any torque produced with no load conditions, but the reason of torque in our case is the compensation of Intertia and Frictional Losses. Thus all the torque produced is utilized against the restrictions, as found in practical motors. The motor as simulated operates at the speed of 700 rev/min. The startup torque and Speed were found to be 28Nm and 880 rev/min respectively.

In figure 30, the torques of individual phases are plotted, where it can be seen that each torque pulse is displaced 30 degrees from other due to the mechanical displacement in the three phases. Inductance profile of each phase is plotted in Figure 31, where the phase shift is also clear to be 30 degrees from each other. The inductance starts from the minimum inductance of L_u and increases to maximum inductance of L_a . For $\beta_r = \beta_s = 30^\circ$, the values for different thetas are given below:

$$\theta_1 = 15 \quad \theta_2 = 45 \quad \theta_3 = 45 \quad \theta_4 = 75 \quad \theta_5 = 90$$

In figure 31, the voltage pulses are also shown. These pulses are the output of the converter, implemented with the help of 'if else' blocks in SIMULINK. As can be seen, the converter supplies $V=150$ for the dwell angle of 10 degrees, and then $V= -150$ for the angle of 30 degrees and finally zero for the other time. The values chosen for the θ_{on} and θ_{off} are good enough since no negative torque is produced. Finally the current of Phase A is plotted to show the maximum current of motor which is almost 10 A.

As can be noted, the SRM torque has a very high torque ripple component which is due to the transitions of the currents from one phase to the following one. This torque ripple is a particular characteristic of the SRM and it depends mainly on the converter's turn-on and turn-off angles.

4.1.2 Simulations with varied θ_{on} and θ_{off}

In this section, different values of theta-on and theta-off are selected and the motor is simulated with no load. The values for the average torque, maximum starting torque, operating speed, and torque ripple are calculated and tabulated in the table. The torque ripple is calculated using equations (5) and (6). The purpose of doing this analysis is to find out the optimum theta-on and theta-off, producing most desirable results. The motor also produces negative torque for some of the values of theta, which are also mentioned in the table.

Table 4: Turn on and Turn off angle Analysis with no load

	Average torque (Nm)	Max starting torque(Nm)	Normal speed (rev/min)	Torque Ripple (%)	Negative Torque
Ton = 20 Toff = 30	1.3164	28.5	660	415.6	No
Ton = 10 Toff = 30	3.008	600	1470	147.34	No
Ton = 0 Toff= 30	4.4719	660	2200	368.6	No
Ton = 20 Toff = 33	1.7968	25	880	261.5	Yes
Ton =20 Toff = 33	1.6118	25	770	309	No
Ton = 10 Toff = 33	3.1320	28	1550	119	No
Ton = 0 Toff = 33	5.1184	300	2500	453	Yes
Ton = 7 Toff = 33	3.73	65	1770	190	No

From the table, it is obvious that for the thetas highlighted Red, negative torque is produced and hence from now on we will discard these values of thetas. The one highlighted in Green have the most favorable results, one producing the torque ripple of 119% and other with that of 181%. For the second value, even the ripple is quite high; we manage to get high average torque and high speed. Thus for now, we will consider both of the values as our optimum results.

The graphs for $\theta_{on}=7$ and $\theta_{off}=33$ are plotted in the following figures.

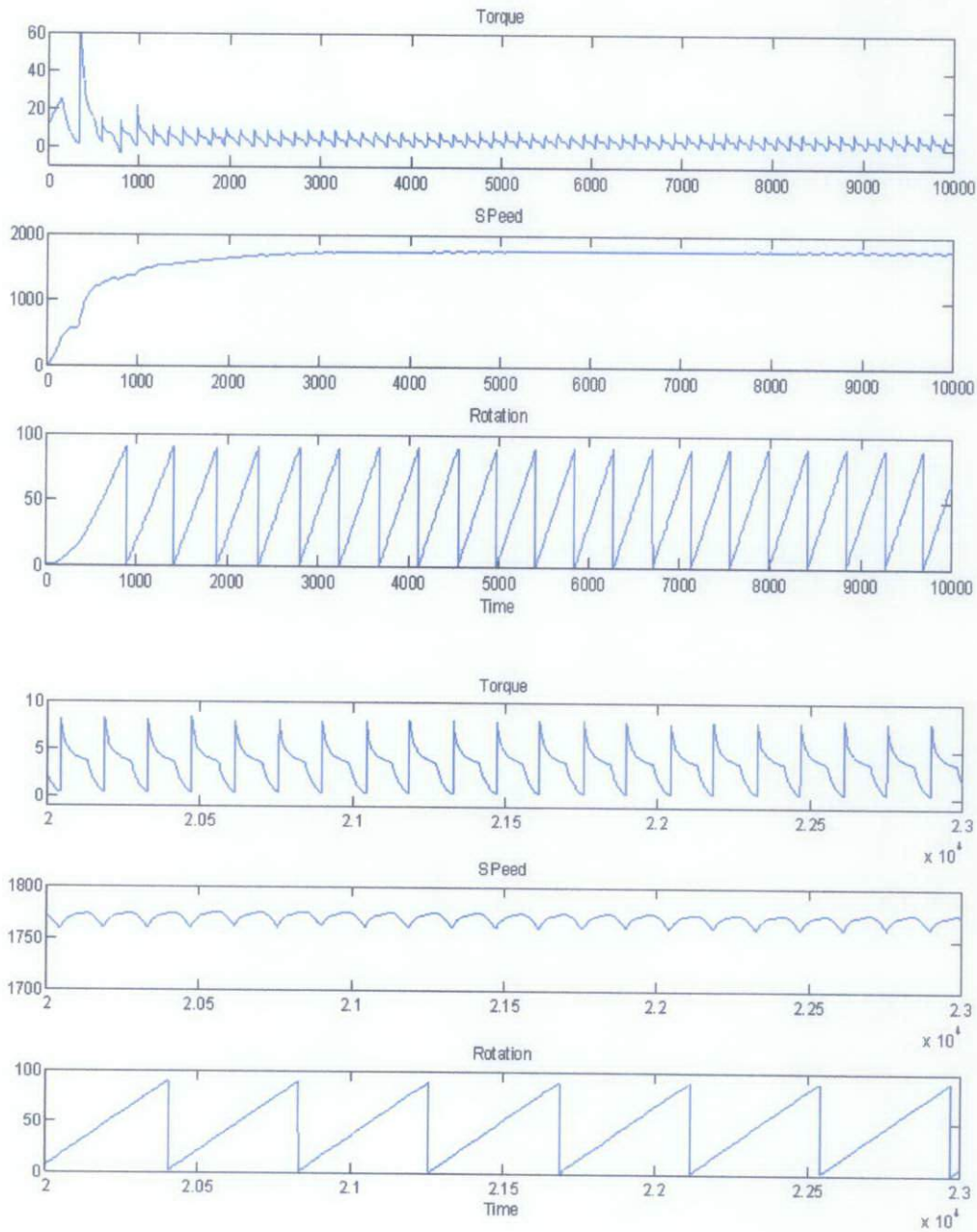


Figure 32: (a) Total Torque, Speed and rotation with $\theta_{on}=7$ and $\theta_{off}=33$, (b) Expanded view of the results simulated in (a)

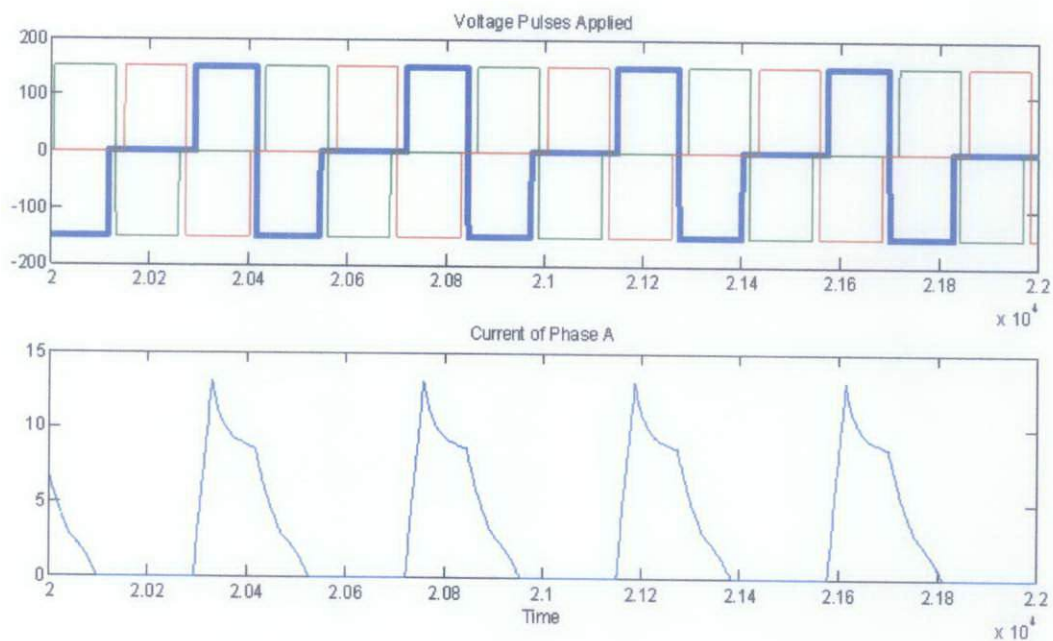


Figure 33: Simulation of Voltage Pulses to individual phases and current of Phase A

It is observed that total current of the motor is increased to $I = 14\text{ A}$ at $\theta_{\text{on}}=7$ and $\theta_{\text{off}} = 33$, from the previous value of $I = 5\text{ A}$ at $\theta_{\text{on}}=20$ and $\theta_{\text{off}} = 30$. The area enclosed by the positive voltage pulse is also increased as can be seen from the figures. At $V=150\text{v}$, the nominal speed obtained from the simulation is 1770 rev/min

4.1.3 Simulation of 6/4 motor with Single Pulse Voltage with Variable Load

In this section, the motor is simulated with variable loads and thus the outputs of average total torque, maximum starting torque and produced speed are calculated and tabulated for different values of θ_{on} and θ_{off} . The purpose of this analysis is to calculate the best values of θ_{on} and θ_{off} as well as to calculate the nominal rated load as well as maximum operating load of the simulated Motor. In our analysis we will apply load on the motor in steps of 5Nm, starting from $T_l = 1\text{Nm}$.

Table 5: Turn on and Turn off angle Analysis with $T_l = 1\text{Nm}$

	Average torque (Nm)	Max starting torque (Nm)	Normal speed (rev/min)	Torque Ripple (%)	Negative torque
Ton = 20 Toff = 30	2.1166	22	550	408.8	N
Ton = 10 Toff = 30	3.7558	75	1280	152.5	N
Ton = 0 Toff = 30	5.1895	650	2000	334.5	N
Ton = 20 Toff = 33	2.3636	25	670	315.5	Y
*Ton = 10 Toff = 33	3.8469	30	1380	135.2	N
Ton = 7 Toff = 33	4.3163	70	1600	200	N

Table 6: Turn on and Turn off angle Analysis with $T_l = 5\text{Nm}$

	Average torque (Nm)	Max starting torque (Nm)	Normal speed (rev/min)	Torque Ripple (%)	Negative torque
Ton = 20 Toff = 30	-	-	-	-	-
Ton = 10 Toff = 30	6.9956	50	900	160	N
Ton = 0 Toff = 30	8.3655	650	1500	365	N
Ton = 10 Toff = 33	7.0737	37	960	132	N
Ton = 7 Toff = 33	7.4347	100	1100	260.3	N

Table 7: Turn on and Turn off angle Analysis with $T_L = 10\text{Nm}$

	Average torque (Nm)	Max starting torque (Nm)	Normal speed (rev/min)	Torque Ripple (%)	Negative torque
Ton = 10 Toff = 30	11.9497	40	700	175.5	N
Ton = 0 Toff= 30	12.6948	750	1150	390.34	N
Ton = 10 Toff = 33	11.4639	55	*760	137.4	N
Ton = 7 Toff = 33	11.8276	100	*860	217.34	N

Table 8: Turn on and Turn off angle Analysis with $T_L = 15\text{Nm}$

	Average torque (Nm)	Max starting torque (Nm)	Normal speed (rev/min)	Torque Ripple (%)	Negative torque
Ton = 10 Toff = 30	15.9857	70	*650	372.37	N
Ton = 0 Toff = 30	17.3408	720	900	412.43	N
Ton = 10 Toff = 33	16.1975	70	*600	153.8	N
Ton = 7 Toff = 33	16.5229	120	*700	242.6	N

In table 5, we can see that there is one value of θ_{on} and θ_{off} , which produces negative torque, and thus we discard it from our further calculations. We can also observe that since for $\theta_{on} = 10$, $\theta_{off} = 30$ and $\theta_{on} = 10$, $\theta_{off} = 33$, produces the best results in terms of average torque and minimum torque ripple. Those two values are highlighted green and are considered optimum values for further calculations.

In table 6, it can be seen that motor could not be operated for the values of $\theta_{on} = 20$ and $\theta_{off} = 30$ with load of $T_L = 5\text{Nm}$. So we will not consider these values anymore. In similar way, the table 7 for load torque $T_L = 10\text{Nm}$ and table 8 for load torque of $T_L = 15\text{ Nm}$ is obtained with the values of maximum speed, average torque and torque ripple produced.

If the torque ripple of all the tables is compared, it would be found out that torque ripple only changes with the values of θ_{on} and θ_{off} , but doesn't depend on the Load. The values for the Nominal speed having asterisk sign (*) in table 7 and table 8 indicates that the speed variation is quite high, where in the average value of speed is noted in the table. This high variation is due to the increase in the Load by keeping the applied voltage constant to $V = 150 \text{ v}$.

After doing the Load Analysis, we can conclude the following things.

1. The motor can be operated at the maximum load of $T_l = 20 \text{ Nm}$ with a lot of variations and fluctuations in speed, but however the rated torque for the motor would be $T_l = 15 \text{ Nm}$.
2. Considering the torque ripple, we can say that, for the values of $\theta_{on} = 10$, $\theta_{off} = 30$ and $\theta_{on} = 10$, $\theta_{off} = 33$, the best torque is produced with the minimum of the torque ripple. We have considered $\theta_{on} = 7$ and $\theta_{off} = 33$ as one of the optimum values, but after the torque ripple analysis and load analysis we can say that it is not as optimum as the other two values.

4.1.4 Implementation of SRM with $\beta_r \neq \beta_s$ (no load) and its Effect

This section focuses on the improvements that are achieved by changing the arc angles of the rotor and stator. In practical motors, the Rotor Arc angle is always greater than that of Stator Arc angle in order for motor to commute better, hence considering that we have simulated the motor with new values of β_s and β_r ($\beta_r \neq \beta_s$) We initially start with $\theta_{on} = 20$ and $\theta_{off} = 30$ and later will do the turn on and turn off angle analysis. We also choose stator arc to be $\beta_s = 24^\circ$ and rotor arc to be $\beta_r = 36^\circ$. It should be kept in mind that since the Aligned Inductance is at $\theta = 51^\circ$ hence we will always keep the θ_{off} less than that value in order for current to reduce to zero before inductance starts to decrease again and produces negative torque.

With the initial values of $\theta_{on} = 20$ and $\theta_{off} = 30$, the torque and speed output for $\beta_r \neq \beta_s$ is same as that of $\beta_r = \beta_s$. Thus only the outputs of individual inductances, current of Phase A and voltage pulses applied are shown in following figures:



Figure 34: (a) Voltage Pulses applied to three phases, (b) Current output of Phase A

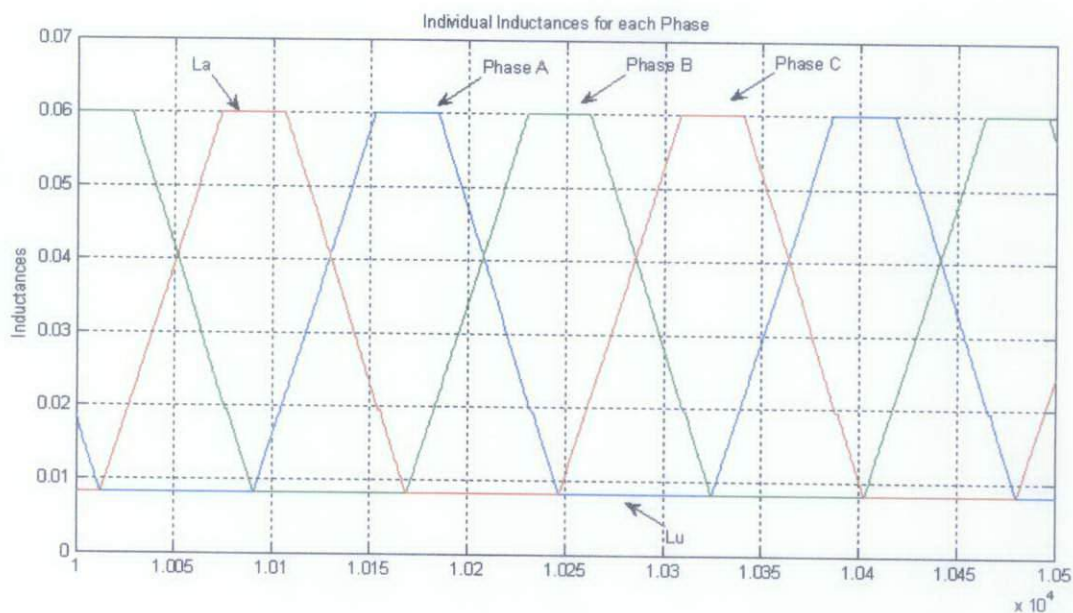


Figure 35: Inductance profile of all the three phases

In figure 35, the inductance of each phase is plotted which seems to have the phase shift of 30 degree. The inductance starts from the minimum inductance of L_u and increases to maximum inductance of L_a . The inductance starts to rise at θ_1 until it reaches θ_2 , where it continues to stay at the maximum inductance until θ_3 and finally it reduces to minimum inductance at θ_4 . For $\beta_s = 24^\circ$ and $\beta_r = 36^\circ$, the values for different thetas are given below:

$$\theta_1 = 15 \quad \theta_2 = 39 \quad \theta_3 = 51 \quad \theta_4 = 75 \quad \theta_5 = 90$$

In figure 34, the voltage pulses applied to the individual phases and phase current are plotted, which are similar to previous graphs.

One of the advantages achieved with variable arcs is that while operating the motor, the turn off angle can be increased without experiencing negative torque, since current will have more time to decrease to zero. This will be further discussed and understood in the theta-on and theta-off analysis.

4.1.5 Simulations with varied θ_{on} and θ_{off} for $\beta_r \neq \beta_s$

In this section, different values of theta-on and theta-off are selected and the motor is simulated with no load. The values for the average torque, maximum starting torque, operating speed, and torque ripple are calculated and tabulated in the table. The purpose of doing this analysis is to find out the optimum theta-on and theta-off, producing most desirable results with $\beta_r \neq \beta_s$. The motor also produces negative torque for some of the values of theta, which are also mentioned in the table.

Table 9: Turn on and Turn off angle Analysis with no load

	Average torque (Nm)	Max starting torque(Nm)	Normal speed (rev/min)	Torque Ripple (%)	Negative Torque
Ton = 20 Toff = 30	1.2314	28.5	650	415.6	No
Ton = 20 Toff = 40	1.6419	25	810	368.6	Yes
Ton = 20 Toff = 35	1.5791	25	800	298.5	No
Ton = 10 Toff = 30	2.9354	800	1400	196.2	No
Ton = 10 Toff = 35	3.0149	27	1500	175.23	No
Ton = 0 Toff = 30	4.7768	800	2100	374.7	No
Ton = 0 Toff = 35	5.8247	400	2200	168.6	Yes

From the table, it is obvious that for the thetas highlighted Red, negative torque is produced and hence from now on we will discard these values of thetas. The one highlighted in Green has the most favorable results, producing the torque ripple of 175%, thus we will consider it as our optimum result. It should be observed that, having rotor and stator arcs equal, the maximum theta-off that could be achieved was 33 degrees but now by increasing the rotor arc, we managed to increase the duty cycle for the torque production.

The graphs for $\theta_{on}=10$ and $\theta_{off} = 35$ are plotted in the following figures.

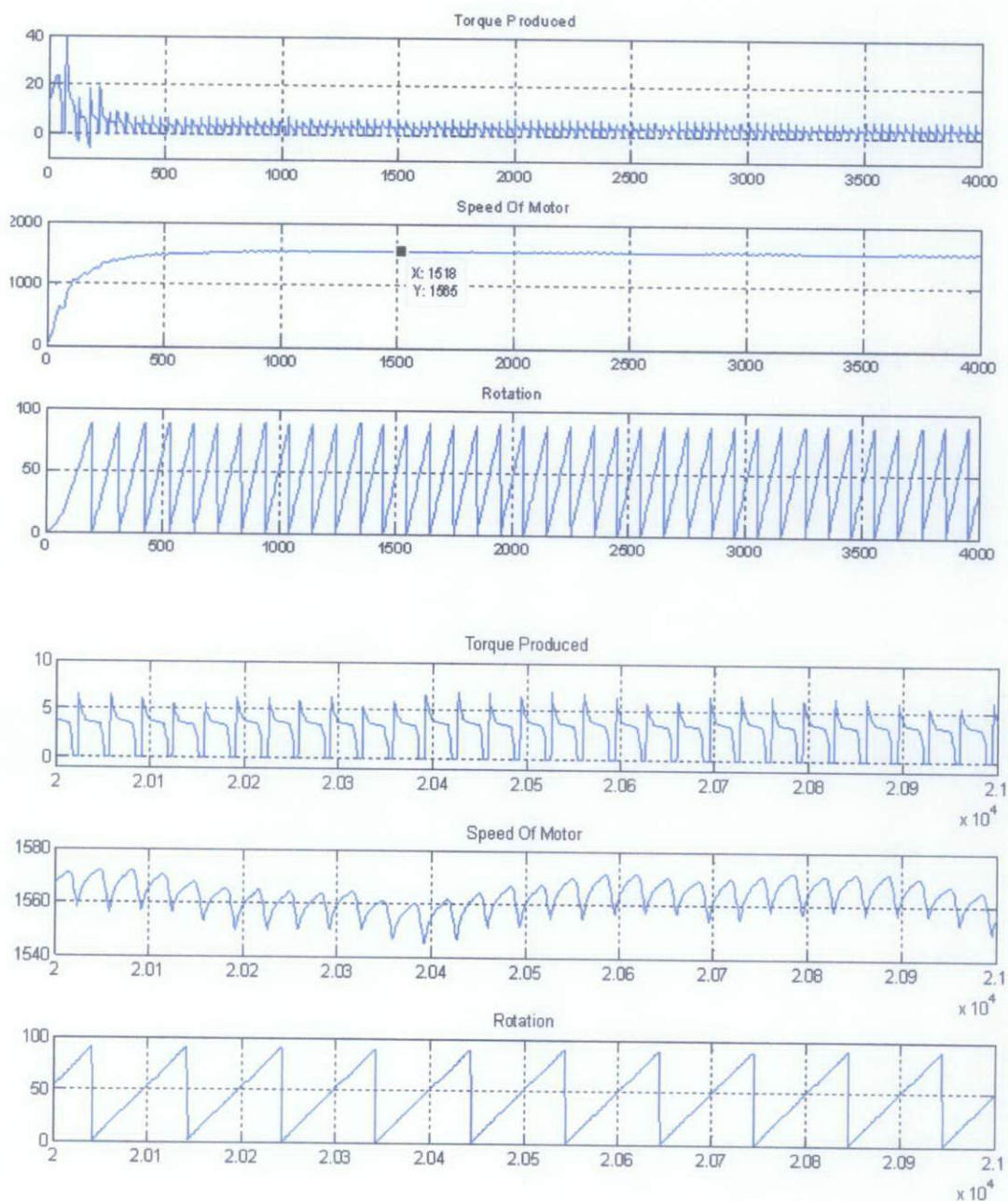


Figure 36: (a) Total Torque, Speed and rotation with $\theta_{on}=10$ and $\theta_{off} = 35$, (b) Expanded view of the results simulated in (a)

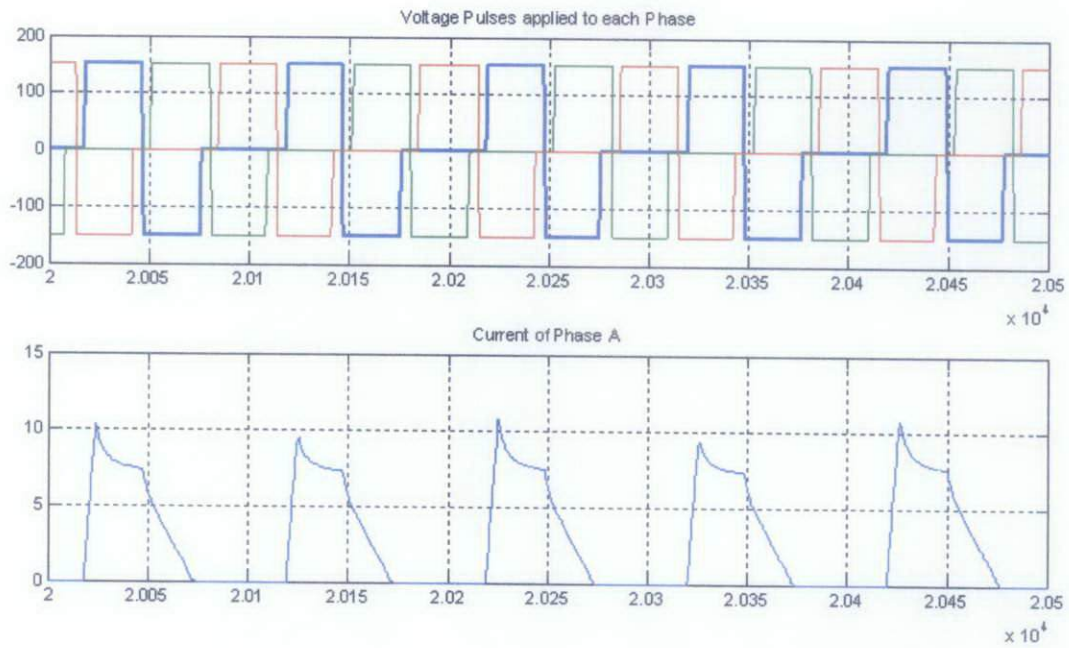


Figure 37: Voltage Pulses to individual phases and current of Phase A

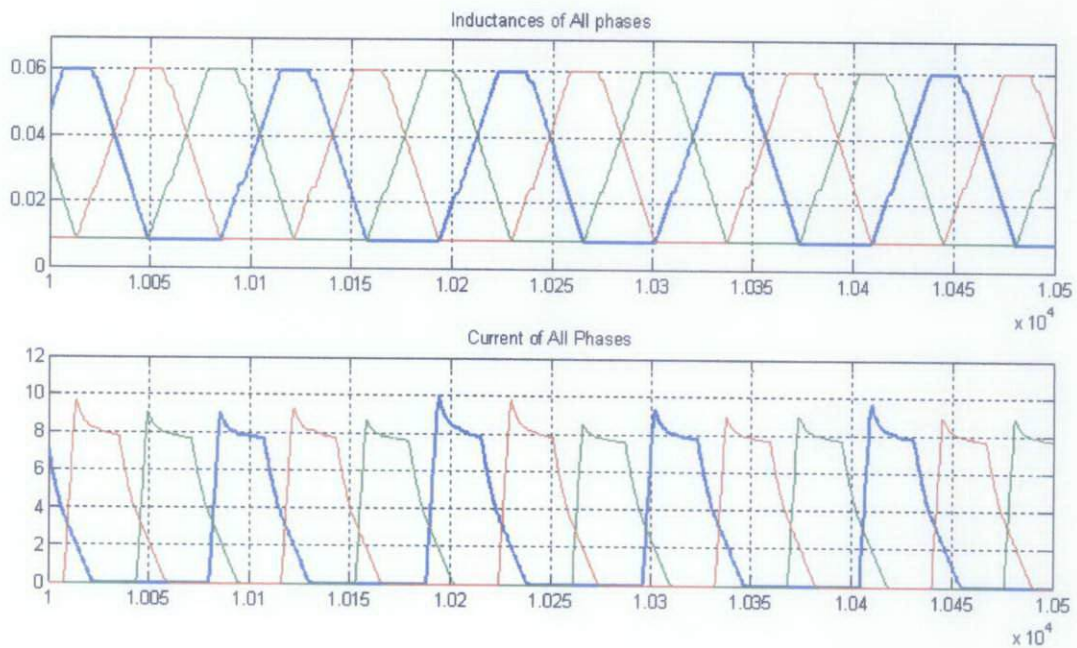


Figure 38: Inductance profile of each phase and Current produced in each phase

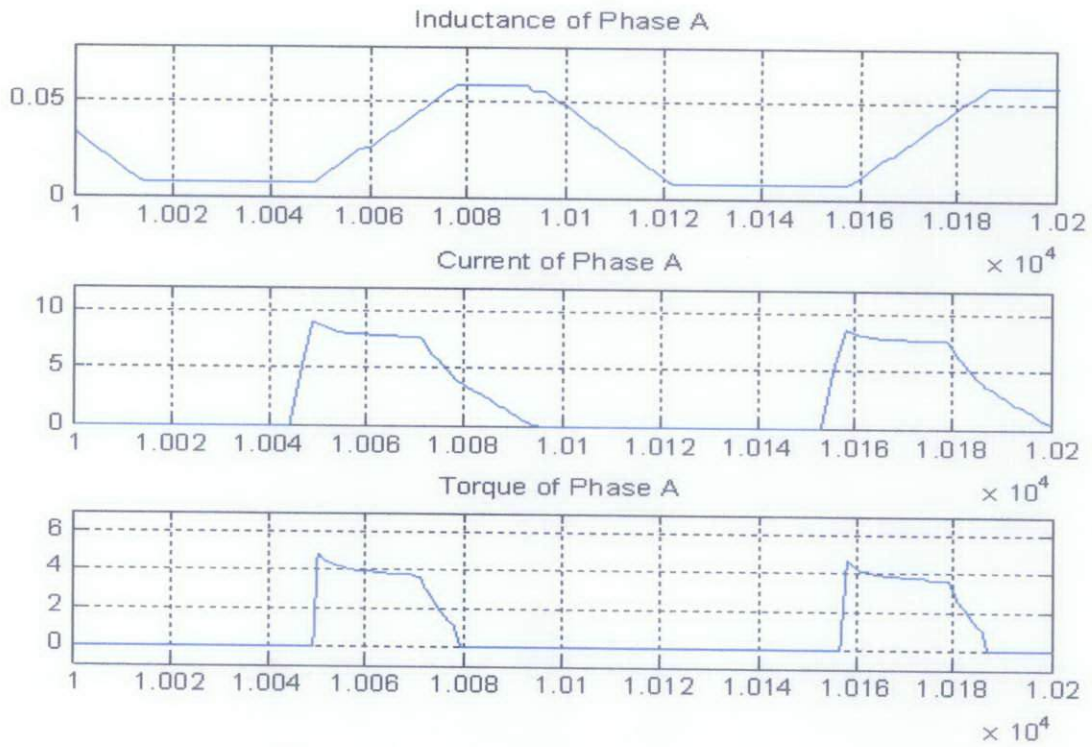


Figure 39: Inductance, Current and Torque of Phase A

Similar to $\beta_r = \beta_s$, the **LOAD ANALYSIS** was done on the motor having unequal stator and rotor pole arcs and thus the outputs of average total torque, maximum starting torque and produced speed were calculated for different values of θ_{on} and θ_{off} . In the experiment, it was found that the values of Theta on equal to 10 degrees and theta off equal to 35 degrees produced the least torque ripple and positive torque. The Normal Rated torque was calculated to be 15 Nm, while the maximum torque was found to be 18 Nm for the optimum theta-on and theta-off, but however the motor failed to operate properly for some of the values of theta

4.1.6 Comparison between motors operated with $\beta_r \neq \beta_s$ and $\beta_r = \beta_s$

The reason of implementing the motor with unequal pole arcs was to obtain better performance results than that of equal pole arcs. The following observations are done after the comparison of two motors:

- For Unequal pole arcs, the graphs are plotted for $\theta_{on}=10$ and $\theta_{off} = 35$ which produce the least torque ripple as was calculated in provided table. These values are selected as optimum values of theta-on and theta-off for the $\beta_r \neq \beta_s$, while for $\beta_r = \beta_s$, the best values were $\theta_{on}=10$ and $\theta_{off} = 33$.
- Usually if the fall angle of current is small, then unequal pole arcs help to improve the average torque and reduce the torque ripples, but in our case, the current took longer time to decrease and hence, only 2 degrees increase (i.e. θ_{off} increased from 33 to 35) in the operating conditions was obtained, considering the fact that greater values produce negative torque.
- Most of the results obtained for different values of theta-on and theta-off for both cases of equal and unequal pole arcs, produced similar results.
- In figure 39, where the torque, inductance and current of phase A is plotted, it can be observed that, the torque is produced for the complete positive slope of inductance and is zero for the dead zone, making torque similar to square pulse. This cannot be achieved from motor with equal pole arcs; where in the current commutation is advanced to some degrees. The action of advanced turn-off reduces the average torque, but in our case, since the total angle of positive slope also decreased, hence there are no observable changes in the average torque with unequal pole arcs.

4.1.7 Simulation of 6/4 motor with Hysteresis Control technique with NO LOAD

To implement hysteresis control or current control, we take produced current as feedback and use it to compare with the reference current. The error produced will trigger the convertor to produce either the positive supply of $V= 150\text{v}$ or negative supply of $V= -150\text{v}$ for each phase. In order to implement the hysteresis in MATLAB, we have used the relay block from library of SIMULINK

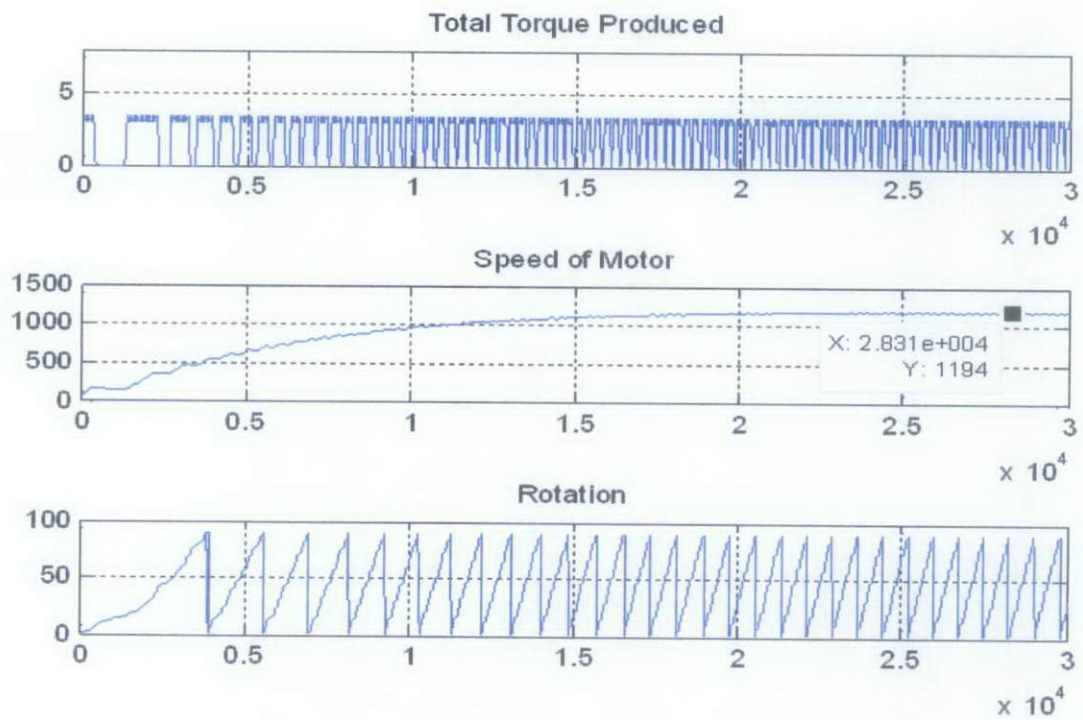
One of the important parameter for hysteresis control is the Hysteresis band denoted by Δe , by which the relay turns on the convertor if the error signal increases above the $\Delta e/2$ value, and turns off the convertor if the error signal decreases below the $-\Delta e/2$ value, while keeping the output constant during the transition. The operation of the hysteresis control can be formulated as below:

$$u_{(t)} = \begin{cases} 0 \longrightarrow e \leq -\frac{\Delta e}{2} \\ 1 \longrightarrow e \geq \frac{\Delta e}{2} \\ u_{(t-\Delta t)} \longrightarrow -\frac{\Delta e}{2} \leq e \leq \frac{\Delta e}{2} \end{cases}$$

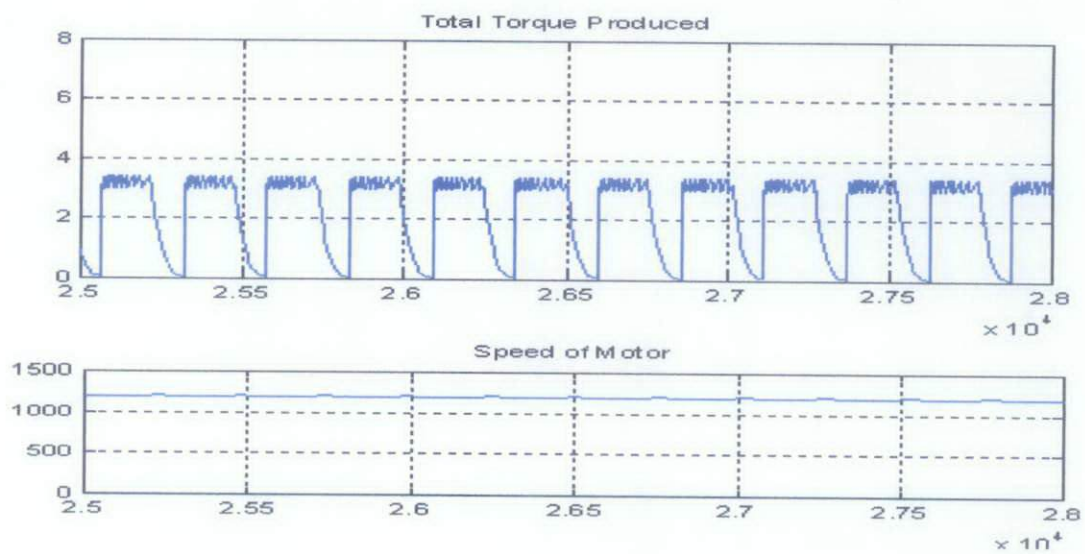
The value of Δe is chosen wisely, because smaller the value, greater will be the switching frequency of the controller and greater will be the cost of operation. Hence for our simulations we have chosen the value of $\Delta e=0.5$.

Using hysteresis control, the reference current has to be manipulated; in our simulations, we have varied the reference current in order to obtain the better performance of the motor.

Initially we choose the turn-on and turn-off angles to be the same as that obtained in last simulations, which were found to be the optimum results. Thus by simulating the motor with $\theta_{\text{on}} = 10$ and $\theta_{\text{off}} = 33$ and keeping rotor and stator arcs equal i.e. $\beta_r = \beta_s = 30^\circ$, we obtained following results:



(a)



(b)

Figure 40: (a) Torque Produced, Speed and Rotation (b) Expanded view of Torque and Speed

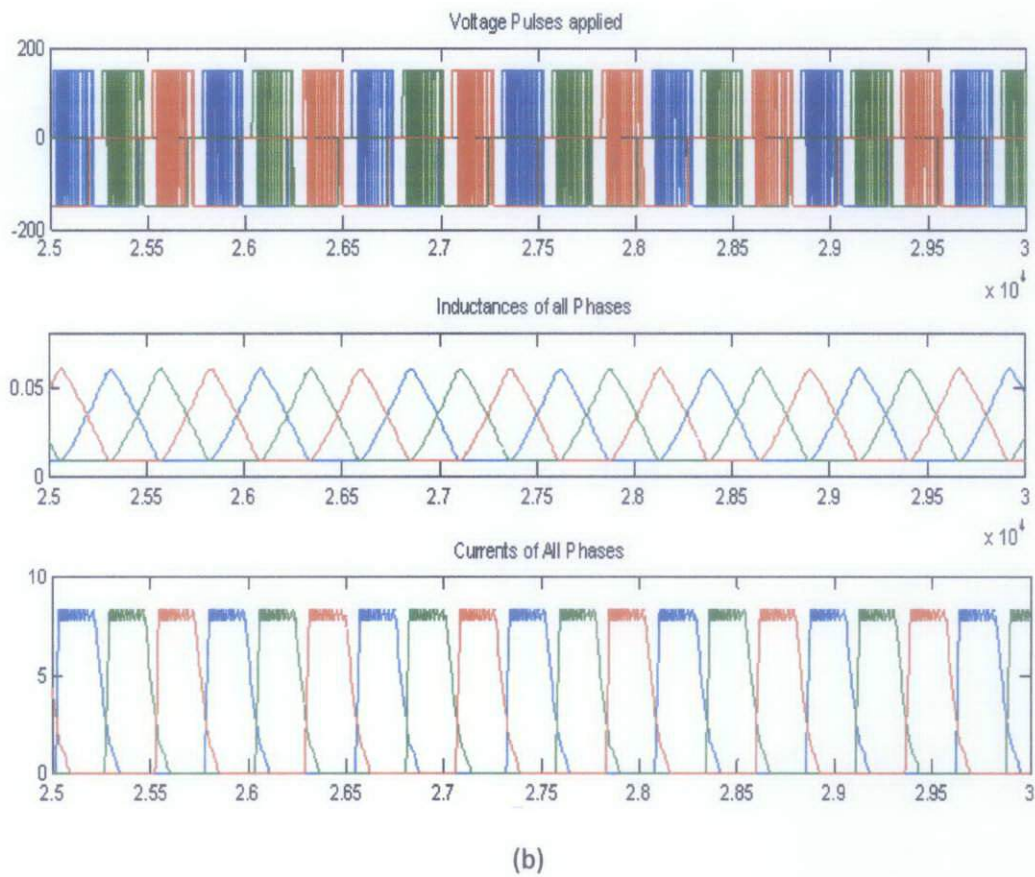
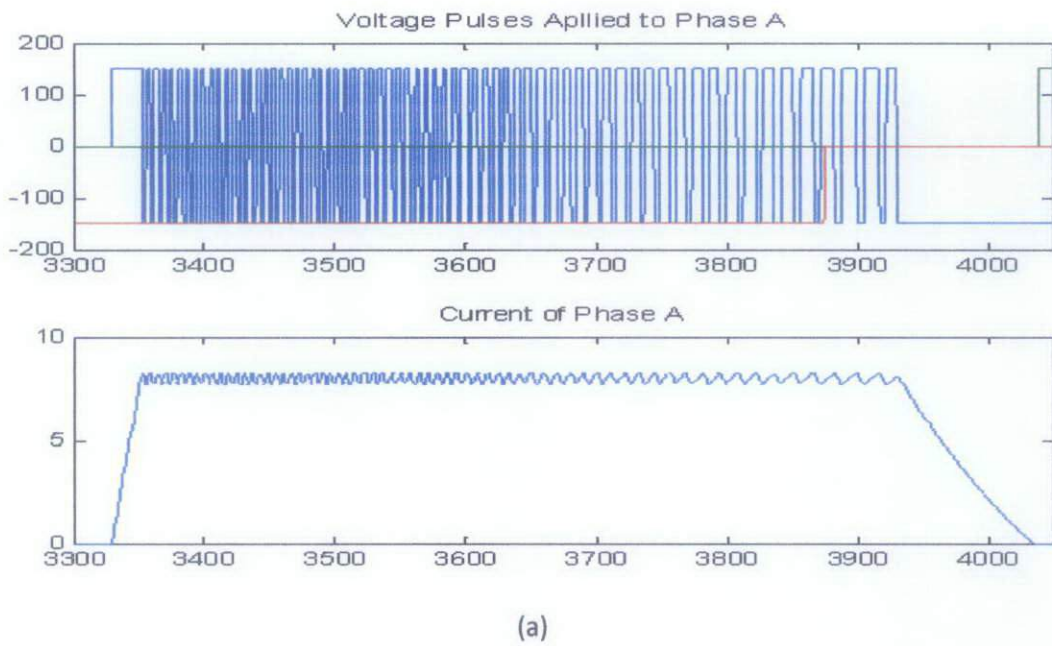


Figure 41: (a) Expanded view of Voltage Pulses applied and Current Produced in Phase A, (b) Voltage pulses applied to all the phases, inductance of all phases and current produced

Interpretation of the Graphs

In above simulation with $\theta_{on} = 10$ and $\theta_{off} = 33$, the reference current was chosen to be $I_{ref} = 8A$ and no load was applied on motor. Usually the hysteresis control is used for low and medium speeds, but in our simulation, due to small value of reference current, the current is controlled throughout the simulation as is observed from graphs.

In figure 40, one can observe the effect of current control on the total torque produced as well as the high torque ripple. It is demonstrated that Maximum torque of 3.5 N.m and Mean torque of 2.2228 N.m is produced with No load. The motor as simulated operates at the speed of 1200 rev/min.

Figure 41, shows the influence of the hysteresis current control on the shape of phase current. Also the switching of power converter is shown, where during hysteresis control, the voltage varies between $+V$ and $-V$. In the hysteresis current control, one can distinguish two methods that allow the current to remain in the hysteresis band: to apply the voltages $+V$ and $-V$ depending on the current error ($I_{ref} - I$) be positive or negative, or apply voltages $+V$ and zero. In the first case, according to the current error, either the IGBTs conduct, or the diodes are conducting. In the second case IGBT Q2 is always open during the regulation phase, while Q1 is blocked or opened according to the error. If Figure 41(a) is observed clearly, one can find that the switching frequency is not constant, it is because that during the faster switching, phase inductance remains constant with its minimum value during 15 deg.

Since a lot of torque ripples are observed, the analysis for turn-on and turn-off angles was performed and the values are calculated and tabulated in the following table

Table 10: Theta on and theta-off analysis for Hysteresis control with no load

	Average torque (Nm)	Ref. Current (A)	Normal speed (rev/min)	Torque Ripple (%)	Negative Torque
Ton = 10 Toff = 33	2.2228	8	1200	147.62	No
Ton = 10 Toff = 33	2.8363	9	1500	127.30	No
Ton = 10 Toff= 33	3.1075	10	1550	116	No
Ton = 10 Toff = 38	3.0053	10	1550	120	Yes
Ton =10 Toff = 37	3.2043	10	1530	112.46	No
Ton = 0 Toff = 37	3.0537	10	1600	118	No

From above table, it is obvious that the value of $\theta_{on} = 10$ and $\theta_{off} = 37$ produce the best results and thus are the optimum values for our simulation. Initially we chose $\theta_{on} = 10$, $\theta_{off} = 33$ and $I_{ref} = 8$ A, later it is observed that, with the increase in reference current, the mean torque increases. At $I_{ref} = 10$ A, the maximum average torque and minimum torque ripple are produced. Thus we changed the operating conditions to $\theta_{on} = 10$ and $\theta_{off} = 37$ and observed that these values produce the highest average torque of 3.2043 Nm and lowest torque ripple of 112.46. For the values of $\theta_{on} = 10$ and $\theta_{off} = 38$, negative torque is experienced thus we neglect these values.

At $I_{ref} = 10$ A, the motor is operated with hysteresis control for low and medium speeds while it is operated with Single Pulse Voltage for higher speeds. If we reduce the reference current, Motor is operated with hysteresis control throughout the simulation. As described earlier, since Hysteresis control is best for medium speeds, we will choose the $I_{ref} = 10$ A as our reference current for Simulation.

In order to do the **Load Analysis**, we will only consider two values of theta-on and theta off i.e. $\theta_{on} = 10$ $\theta_{off} = 37$ and $\theta_{on} = 0$ $\theta_{off} = 37$. It should also be noted that since the Motor needs higher current for producing higher torque, reference current should be increased with the increase in load.

Table 11: Theta on and theta-off analysis for Hysteresis control with $T_l=1Nm$

	Average torque (Nm)	Ref. Current (A)	Normal speed (rev/min)	Torque Ripple (%)	Negative Torque
Ton = 10 Toff = 37	3.7090	10	1400	93.13	No
Ton = 10 Toff = 37	4.1404	14	1500	132.7	No
Ton = 0 Toff= 37	3.6239	10	1400	115.9	No
Ton = 0 Toff= 37	3.8971	12	1500	107.8	No

Table 12: Theta on and theta-off analysis for Hysteresis control with $T_l=5Nm$

	Average torque (Nm)	Ref. Current (A)	Normal speed (rev/min)	Torque Ripple (%)	Negative Torque
Ton = 10 Toff = 37	7.0308	14	1000	89.6	No
Ton = 10 Toff = 37	7.2549	17	1000	88.2	No
Ton = 0 Toff= 37	6.6059	14	1000	97.05	No
Ton = 0 Toff= 37	6.8065	17	1100	163.4	No

Table 13: Theta on and theta-off analysis for Hysteresis control with $T_l=10\text{Nm}$

	Average torque (Nm)	Ref. Current (A)	Normal speed (rev/min)	Torque Ripple (%)	Negative Torque
Ton = 10 Toff = 37	11.6345	20	800	90.31	No
Ton = 10 Toff = 37	11.6427	23	800	91.2	No
Ton = 0 Toff = 37	10.6699	20	800	122	No
Ton = 0 Toff = 37	10.7658	21	800	145	Yes

After the Load analysis, following things can be concluded:

- With Hysteresis control, Less Torque ripple is Possible.
- Increase in reference current increases the torque ripple but also increase the mean torque.
- The rated nominal torque for simulated motor is $T_l=15\text{ Nm}$ at the reference current of $I_{ref}= 25\text{ A}$. However the motor can be operated up to the maximum load torque of $T_l=20\text{Nm}$ at $I_{ref}= 28\text{ A}$.

For the comparison of motor values for the Voltage control and Current Control, refer to the table below

Table 14: Comparison of two control techniques for $T_l=10\text{Nm}$

Optimum values of Theta-on and theta-off	Mean torque	Speed	Torque Ripple
Ton = 10 Toff = 33	11.4639	760	137.4
Ton = 10 Toff = 37	11.6427	800	91.2

After all the analysis done with the 6/4 SRM, it is concluded that, the motor can be controlled with either Single Pulse Voltage Technique or Current Control Technique. Various calculations were performed in order to obtain the optimum values for theta-on and theta-off with and without Load. The motor was implemented with equal as well as unequal pole arcs.

After all these simulations and analysis, it can be declared that the dwell angle can be increased with unequal pole arcs and hence the mean torque can be increased. Dwell angle can also be further increased with implementation of Hysteresis and Voltage pulse technique together, which ultimately produces the higher mean torque and lower torque ripple. From Table 14, it can be seen that, for the Load of $T_l = 10 \text{ Nm}$ and $\beta_r = \beta_s$, dwell angle for Voltage control technique is smaller than that of Hysteresis control and as a result, mean torque produced is small.

With regard to the turn-on angle, it is recommended to anticipate its value to the moment where phase inductance begins to increase, to be able to take advantage of a high di/dt . However, it is proper to notice that if one applies the turn-on angle too early, we will be in a region where the inductance change in relation to the rotor position is small, thus the produced torque will be small as well as the current will be high, increasing the power losses. Hence, it is necessary to choose an appropriate value to μ_{on} if one wants to optimize the motor efficiency. It is also observed that with voltage control the speed starts to oscillate with Load, but however such effect is very rare in Hysteresis control. Torque ripple produced by Hysteresis control is the minimum among all the calculations for Voltage Pulse.

4.2 Simulation of 8/6 SRM

This motor has four phases and eight stator poles, while six rotor poles. The phases are independent from each and are similar to other but are only mechanically shifted from each other for an angle called Step angle or transition angle given by:

$$\theta_s = 2\pi \left(\frac{1}{N_r} - \frac{1}{N_s} \right)$$

The Step angle was calculated to be 15 degrees. Each phase of the motor needs to be energized at least once in order to move the rotor by 60 degrees, thus in order to complete one revolution of the motor, each phase has to be energized 6 times. ($60 \times 6 = 360$). The complete simulation of the 8/6 SRM is given in following figure.

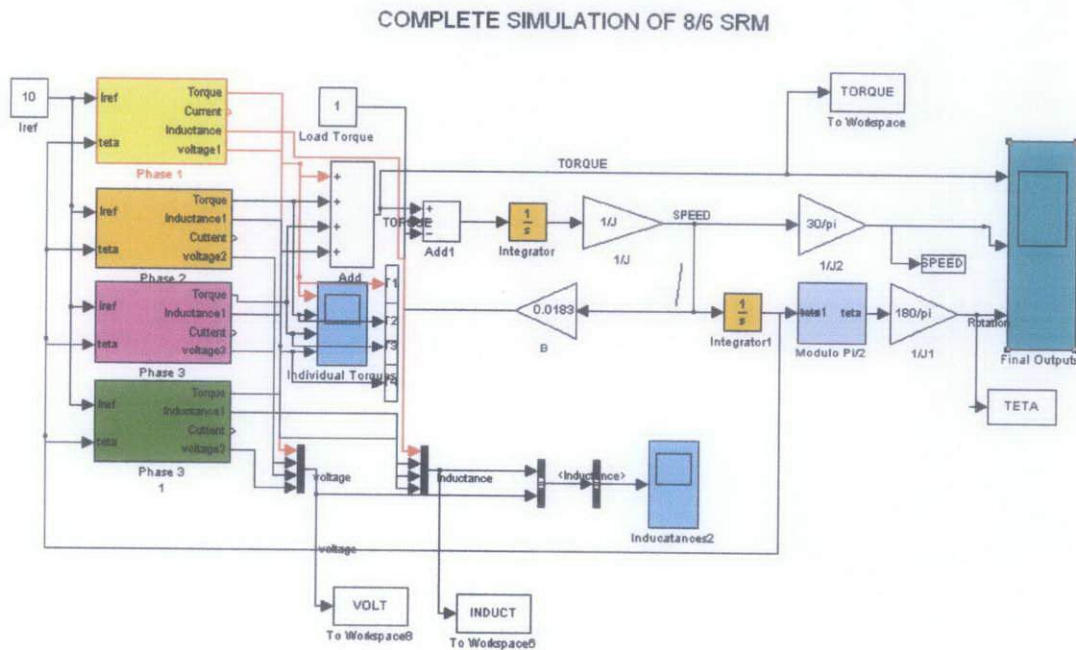


Figure 42: Complete Simulation Model of 8/6 SRM

As can be observed, the simulation is similar to 6/4 SRM, with the addition of one more phase. Each phase is fed back with the input of Position of the rotor and the reference current that is used for the hysteresis purposes. Each phase produces torque pulse, which are added together to make total torque of motor. The output of total torque, speed and position is measured and displayed using scope. Further the outputs like phase current, phase inductance, phase flux as well as phase voltages are calculated and obtained using Scope in SIMULINK.

In order to have insight of the phases of 8/6 SRM, one can refer to simulation of 6/4 SRM, since phases are simulated with similar methods. However there are some changes in the simulation which are discussed below:

- Modulo block in each phase is no longer Modulo $\pi/2$, instead since the phases have to be energized after every 60 degrees, thus it is modulo $\pi/3$ block now.
- For each phase shift we will use the following equation. In order to implement the phase shifts we have modified the Modulo block of each phase.

$$shift = \theta + (n - i - 1)\theta_s \text{ Where } n = N_r = 4 \text{ and } i = 1, 2, 3, 4$$

Thus For

$$I=1 \text{ Phase shift} = \theta + 2\theta_s$$

$$I=2 \text{ phase shift} = \theta + \theta_s$$

$$I=3 \text{ phase shift} = \theta,$$

$$I=4 \text{ phase shift} = \theta - \theta_s$$

- Also the inductance profile will be different for 8/6 motor, since the thetas ($\theta_1, \theta_2, \theta_3, \theta_4$ and θ_5) would be different from that of 6/4 Motor. The details of which could be found in Appendix II

4.2.1 Simulation of 8/6 motor with Single Pulse Voltage technique with little LOAD

Initially we choose $\theta_{on} = 5$ and $\theta_{off} = 18$ and we keep rotor and stator arcs equal i.e. $\beta_r = \beta_s = 15^\circ$. The values of θ_{on} and θ_{off} are chosen randomly to check the performance of motor. It should be kept in mind that since the Aligned Inductance is at $\theta = 30^\circ$ hence we will always keep the θ_{off} less than that value in order for current to reduce to zero before inductance starts to decrease again and produces negative torque.

Following graphs are obtained with the simulation of the motor when Load $T_l = 1\text{Nm}$ is applied.

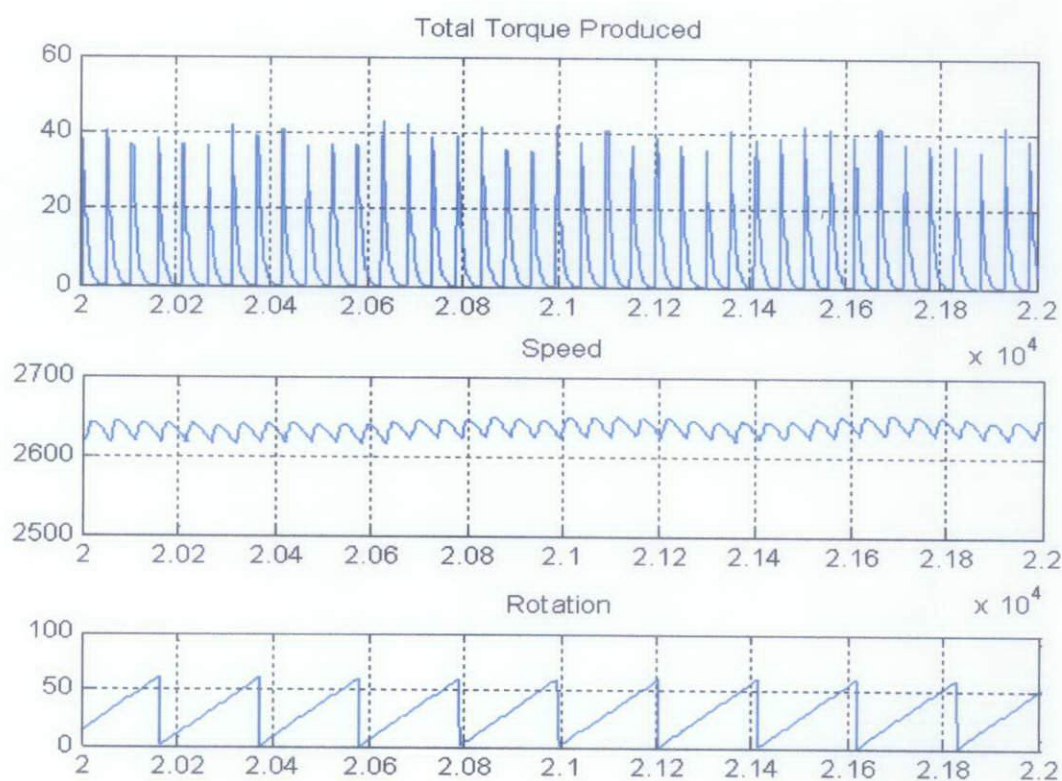
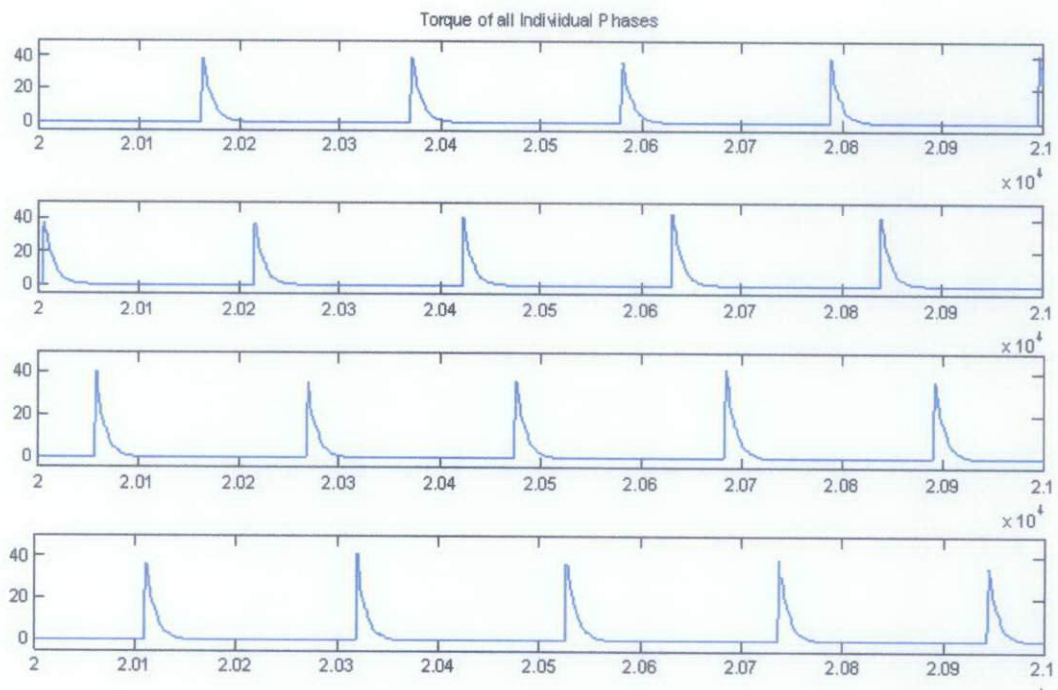
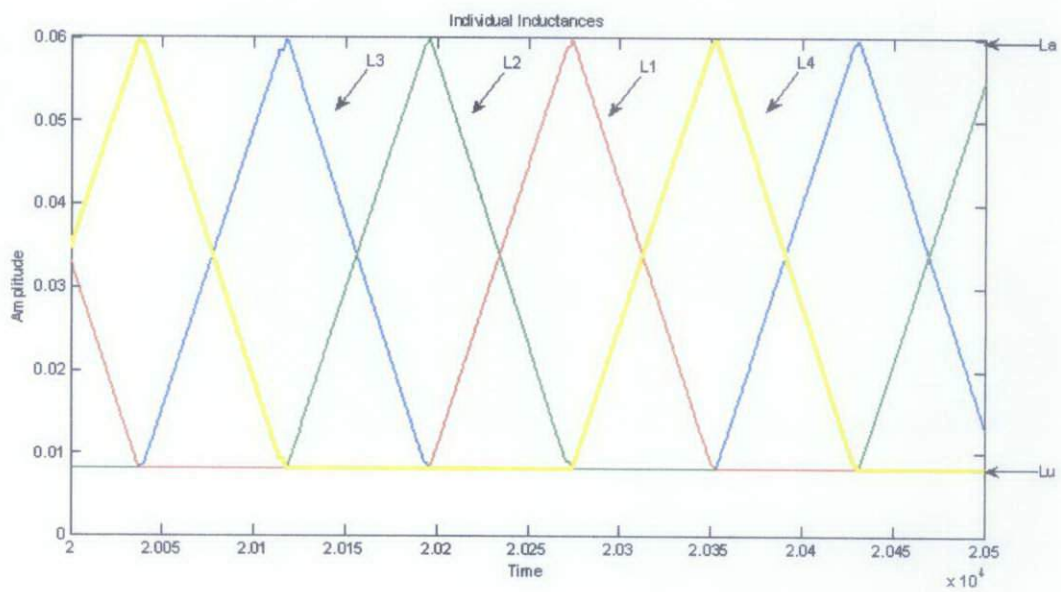


Figure 43: Output of Total Torque, Speed and rotation of 8/6 Motor with little load

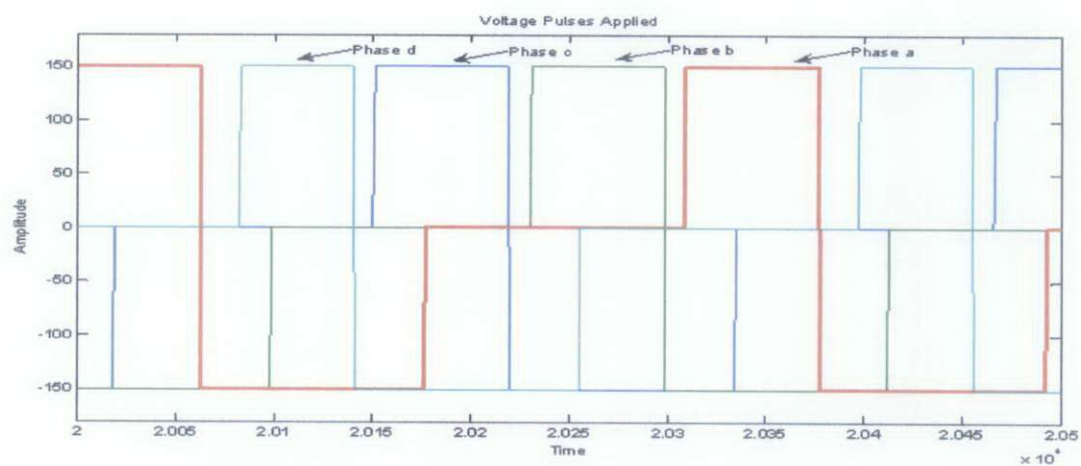


(a)

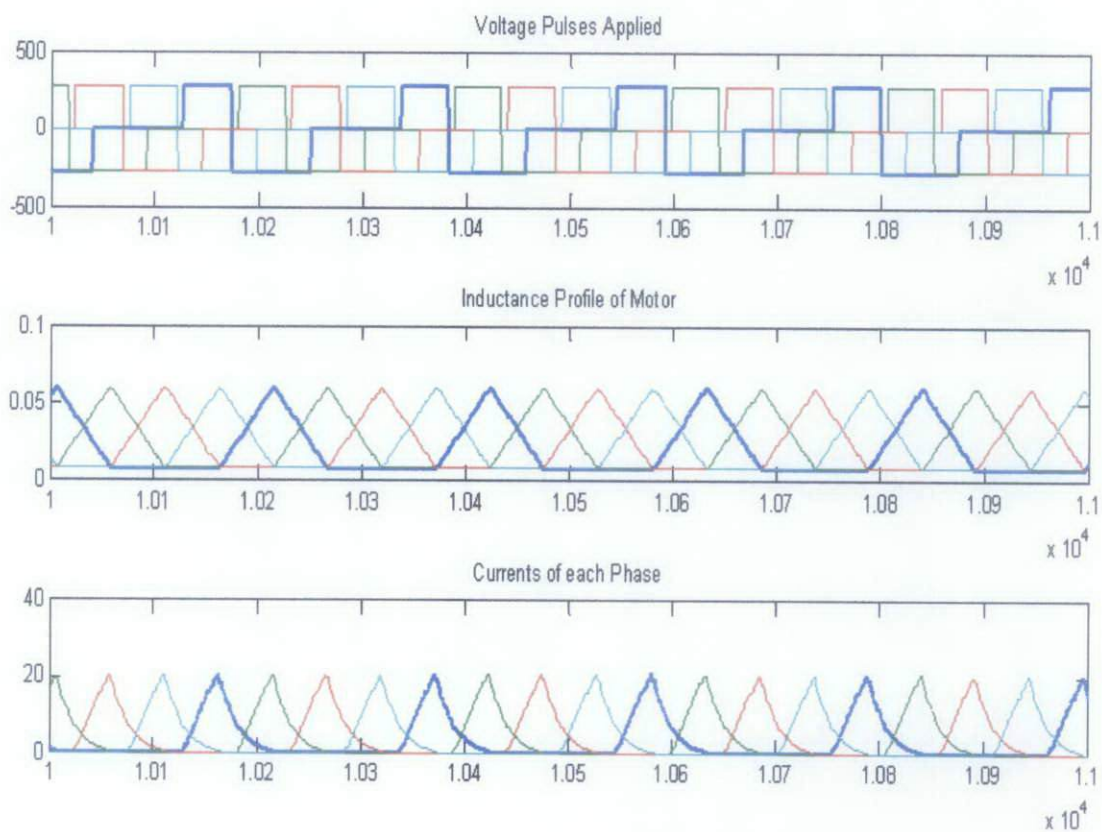


(b)

Figure 44: (a) Expanded view of Individual Torques generated from each phase, (b) Individual Phase Inductances



(a)



(b)

Figure 45: (a) Expanded view of Individual Voltage Pulses Applied, (b) Voltage Pulses, Phase Inductances and Phase Currents produced

Interpretation of Graphs

In figure 43, it is demonstrated that Maximum torque of 40 N.m, Mean torque of 7.2128 N.m and speed of 2630 rev/min is produced with load of $T_l = 1\text{Nm}$. The SRM simulation using its linear model needs to consider the initial rotor position. If the rotor is at the region where inductance has the constant value, then no torque will be produced. Hence if the load torque is zero, machine will be halted for all the time. In our simulation, we have not assigned any initial rotor position, however we have given the load of $T_l = 1\text{Nm}$, through which machine starts to rotate.

In figure 44 (a), the torques of individual phases are plotted, where it can be seen that each torque pulse is displaced 15 degrees from other due to the mechanical displacement in the three phases. Inductance profile of each phase is plotted in figure 44 (b), where the phase shift is also clear to be 15 degrees from each other. The inductance starts from the minimum inductance of L_u and increases to maximum inductance of L_a . For $\beta_r = \beta_s = 15^\circ$, the values for different thetas are given below:

$$\theta_1 = 15 \quad \theta_2 = 30 \quad \theta_3 = 30 \quad \theta_4 = 45 \quad \theta_5 = 60$$

In figure 45(a), the voltage pulses are shown. These pulses are the output of the converter, implemented with the help of 'if else' blocks in SIMULINK. As can be seen, the converter supplies $V=280$ for the dwell angle of 13 degrees, and then $V= -280$ for the angle of 22 degrees and finally zero for the other time. The values chosen for the θ_{on} and θ_{off} are good enough since no negative torque is produced. Finally the current of all the phases is plotted in figure 45(b) to show the maximum current of motor which is almost 20 A.

4.2.2 Simulations with varied θ_{on} and θ_{off} and variable Load

In this section, different values of theta-on and theta-off are selected and the motor is simulated with load of 1Nm. The values for the average torque, maximum starting torque, operating speed, and torque ripple are calculated and tabulated in the table. The purpose of doing this analysis is to find out the optimum theta-on and theta-off, producing most desirable results. The motor also produces negative torque for some of the values of theta, which are also mentioned in the table.

Table 15: Turn on and Turn off angle Analysis with load $T_l=1\text{Nm}$

	Average torque (Nm)	Normal speed (rev/min)	Torque Ripple (%)	Negative Torque
Ton = 5 Toff = 18	7.2128	2630	593.47	No
Ton = 10 Toff = 20	5.0185	1920	473.5	No
Ton =10 Toff= 25	5.5761	2200	228.25	No
Ton = 0 Toff = 25	Unstable	Unstable	Unstable	Yes
Ton =5 Toff = 25	----	3700	----	Yes

Table 16: Turn on and Turn off angle Analysis with load $T_l=5\text{Nm}$

	Average torque (Nm)	Normal speed (rev/min)	Torque Ripple (%)	Negative Torque
Ton = 5 Toff = 18	10.4103	2100	558.06	No
Ton = 10 Toff = 20	7.9437	1500	420.58	No
Ton =10 Toff= 25	8.8106	1700	240.87	No

Through these simulations we have found out that, at $\theta_{on}=10$ and $\theta_{off}=25$ degrees produce the best result in terms of mean torque and torque ripple with no negative torque. The rated nominal torque of the motor is calculated to be 35 Nm.

If these calculations are compared with that of 6/4 motor, we will find that, we have managed to achieve higher mean torque, higher speeds and low oscillations as well as higher rated torque with almost equal torque ripples.

After simulating 8/6 motor with equal pole arcs with voltage pulse technique and doing load analysis, we observed that, the results are very much improved in terms of mean torque. Only the torque ripple is slightly higher than that of 6/4 motor. Thus in order to compensate for that, we will do our final simulation of 8/6 motor using hysteresis control technique.

The values calculated are tabulated in following tables.

Table 17: Hysteresis control technique

	Average torque (Nm)	Normal speed (rev/min)	Refernce Current (A)	Torque Ripple (%)	Negative Torque
Ton = 5 Toff = 18	2.2760	1200	12	586.44	No
Ton = 10 Toff = 20	3.1779	1500	10	289.78	No
Ton =10 Toff= 20	3.7602	1600	12	347.35	No
Ton =10 Toff= 25	5.1499	2100	12	205.5	No
Ton =10 Toff= 25	4.4447	1900	10	143.81	No

It should be observed from the above table that even the speed as well as mean torque increases with increase in reference current, but torque ripple also increases which is undesirable. So we have to choose the parameter of output mean torque and torque ripple in our simulation. This effect was not observed in 6/4 motor, where in increase in reference current increase decreased the torque ripple. Thus from our simulation we have obtained the minimum torque ripple for reference current of $I = 10\text{ A}$ and $\theta_{on}=10$ and $\theta_{off}=25$ degrees.

From all the simulations done on SRM we can conclude that the motor can be operated on different theta-on and theta-off values, but selection of optimum values is necessary to produce the better results. Also improvement in torque ripple, mean torque, average speed and dwell angle was obtained with the implementation of Hysteresis control as compared with Single Pulse Voltage Technique.

Some of the results for Hysteresis control for 8/6 SRM are plotted here:

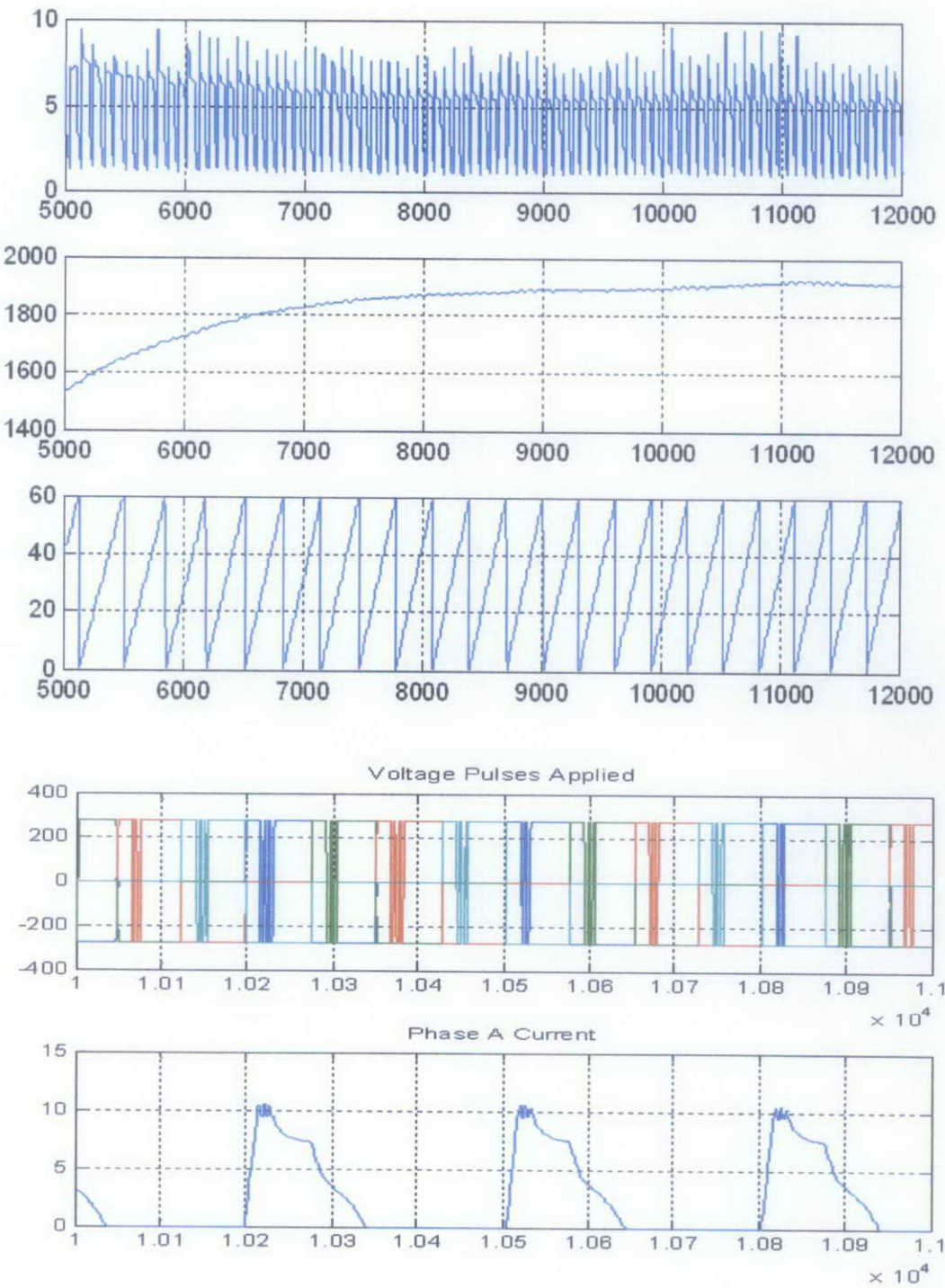


Figure 46: Hysteresis control of SRM

CHAPTER 5

CONCLUSION AND RECOMMENDATIONS

5.1 Conclusion

In this project the author went through organized set of stages to reach his desired results starting from literature review and study of various techniques that have been used for the improvement of the performance of the Switched Reluctance Motor. SRM offer some advantages along with potential low cost, for example, they can be very reliable machines since each phase of the SRM is largely independent physically, magnetically, and electrically from the other motor phases. Also, because of the lack of conductors or magnets on the rotor, very high speeds can be achieved, relative to comparable motors. SRM have some disadvantages like they are difficult to control, they are noisy and they have more torque ripple than other types of motors. But the performance can be improved with better understanding of SRM mechanical design and the development of algorithms that can compensate for these problems.

SRM is simulated and observed using the Library model available in MATLAB to produce the torque and speed. It was observed that the Torque Produced has many ripples and they degrade the performance of Motor.

Later Switched Reluctance Motor was simulated in SIMULINK with two different configuration i.e. 6/4 and 8/6. The control techniques of Single Pulse and Hysteresis control were implemented on motor and parameters like Mean torque, operating speed and torque ripple were calculated and plotted.

Finally, optimum values of turn-on and turn-off thetas were calculated with load and without load and the best results with highest mean torque and lowest torque ripple were obtained. Torque Ripple was decreased considerably after the implementation of Hysteresis Control, also there was increase in mean torque, speed and dwell angle for the SRM

5.2 Recommendations

This project and thesis can help to understand the working of the Switched Reluctance Motor and understand its various configurations. It also covers the control modeling of SRM using Simulink, which could be understood and implemented. The control techniques have improved the torque ripple considerably, but in order to further improve the performance, other techniques like Bacteria Foraging Algorithm can be applied. BFA is a genetic algorithm, which have been used widely to optimize the performance of different processes.

REFERENCES

- [1] Mehran Rashidi, Farzan Rashidi, Mohammad Hossein Aghdaei, & Hamid Monavar "*Speed Control and Torque Ripple Minimization in Switch Reluctance Motors using Context based Brain Emotional learning*" M.G h. Negoita et al. (Eds.): KES 2004, LNAI 3215, pp. 278–284, 2004.
- [2] Majid Hajatipour a, Mohammad Farrokhi a,b,* "*Adaptive intelligent speed control of switched reluctance motors with torque ripple reduction*" accepted 29 September 2007 by Energy Conversion and Management.
- [3] Aras Sheikhi, Hashem Oraee, Shahriyar Kaboli, Mohammadreza Dorkhah, "*A new configuration of Switched Reluctance Motor for reducing the torque ripple*".
- [4] Nihat Inanc "*Phase current modulation of switched reluctance motor to minimize torque ripple*" accepted 16 October 2001 by Electric Power Systems Research.
- [5] Michael T. DiRenzo "*Switched Reluctance Motor Control – Basic Operation And Example Using The Tms320f240*" Application Report SPRA420A - February 2000, published by Texas Instruments
- [6] T. Datta and I. S. Misra , B. B. Mangaraj, S. Imtiaj "*Improved Adaptive Bacteria Foraging Algorithm In Optimization Of Antenna Array For Faster Convergence*" *Progress In Electromagnetics Research C*, Vol. 1, 143–157, 2008
- [7] A.Anuradha "Analysis of Dynamic Charactersistics of Switched Reluctance Motor based on MATLAB/SIMULINK"
- [8] Reston Condit (Microchip Technology Inc.), Dr. Douglas W. Jones (University of Iowa) "Stepping Motor Fundamentals", 2004 Microchip Technology Inc.
- [9] Kevin M. Passino "*Biomimicry of Bacterial Foraging for Distributed Optimization and Control*" IEEE Control Systems Magazine, June 2002
- [10] H. Berg, "*Motile behavior of bacteria,*" *Phys. Today*, pp. 24-29, Jan. 2000.

- [11] Vikas S. Wadnerkar, Dr. G. TulasiRam Das, Dr. A.D. Rajkumar, "Performance analysis of Switched Reluctance Motor; Design, modeling and simulation of 8/6 SRM" *Journal of Theoretical and Applied Information Technology*, 2005 - 2008 JATIT.
- [12] P. J. Lawrenson, J. M. Stephenson, P. T. Blenkinsop, J. Corda and N. N. Fulton, "Variable-speed switched reluctance motors," *IEE Proceedings Part-B*, Vol. 127, No. 4, July 1980, pp. 253-265.
- [13] F. Soares P. J. Costa Branco Instituto Superior T'ecnico Portugal "Simulation of a 6/4 Switched Reluctance Motor based on MATLAB/SIMULINK environment"
- [14] Implementation of a Current Controlled Switched Reluctance motor using TMS320F240, application report: SPRA 282.
- [15] N.J. Nagel and R.D. Lorenz " Modeling of a Saturated Switched Reluctance Motor Using an Operating Point Analysis and the Unsaturated Torque Equation", In Proc. Of IEEE, IAS Annual Conf., Oct. 3-7, 1999, Phoenix, pp. 2219-2226.
- [16] Shoujun Song & Weiguo Liu School of Automation, Northwestern Polytechnical University "A Comparative Study on Modeling Methods for Switched Reluctance Machines" Vol. 3, No. 2; May 2010.
- [17] Ercument Karakas^{1,*} and SONER VARDARBASI² "Speed control of SR motor by self-tuning fuzzy PI controller with artificial neural network" *S⁻adhan⁻a* Vol. 32, Part 5, October 2007, pp. 587-596. © Printed in India
- [18] P. Brandstetter, R. Hrbac, M. Polak, L. Stepanec "Application Of Fuzzy Logic In Control Of Switched Reluctance Motor" *Advances in Electrical and Electronic Engineering*
- [19] X. D. Xue, K. W. E. Cheng, J. K. Lin, Z. Zhang, K. F. Luk, T. W. Ng, and N. C. Cheung "Optimal Control Method of Motoring Operation for SRM Drives in Electric Vehicles" *IEEE Transactions on vehicular technology*, vol. 59, no. 3, march 2010

APPENDIX I
Project Gantt Chart

			Planned		Week														
#	List of Activities	Start	Duration	1	2	3	4	5	6	7	8	9	10	11	12	13	14	15	
1	LITERATURE REVIEW																		
1.1	Word recognition	Week 1	3 weeks																
1.2	Speaker Recognition	Week 3	3 weeks																
2	DESIGN & DEVELOPMENT OF SPEAKER RECOGNITION																		
2.1	Voice Activity Detection (VAD)	Week 5	2 weeks																
2.2	Spectral Subtraction (SS)	Week 5	2 weeks																
2.3	Mel-Frequency Cepstrum Coefficient (MFCC)	Week 6	2 weeks																
2.4	Dynamic Time Warping (DTW)	Week 6	2 weeks																
2.5	Word Recognition	Week 7	2 weeks																
2.5	Vector Quantization (VQ)	Week 7	4 weeks																
2.6	Speaker Recognition																		
2.7	Combination of Word and Speaker Recognition	Week 8	3 weeks																
2.8	Improvement																		
3	PROGRESS REPORT WRITE-UP	Week 7	1 week																
4	TECHNICAL REPORT WRITE-UP	Week 8	2 weeks																
5	POSTER PREPARATION FOR EDX	Week 9	1 week																
6	INTERIM REPORT FINAL DRAFT WRITE-UP	Week 11	2 weeks																
7	ORAL PRESENTATION	Week 14	1 week																

APPENDIX II

Simulation Initializations

Initialization for 6/4 motor with equal betas

```

NS=6          ;          %No. of Stator Poles
NR=4          ;          %No. of Rotor Poles
P=3;

BETAS = 30*(pi/180);      % angle of the arc of stator
BETAR = 30*(pi/180);      %angle of the arc of rotor
TETAS = (2*pi)*((1/NR)-(1/NS)); % Step angle per transition
%%%%%%%%%%%%%%%%%%%%%%%%%%%%%%%%%%%%%%%%%%%%%%%%%%%%%%%%%%%%%%%%%%%%%%%%
TETAX = (pi/NR)-((BETAR+BETAS)/2);      % tetax = 15 degrees
TETAY = (pi/NR)-((BETAR-BETAS)/2);      % tetay = 45 degrees
TETAZ = (BETAR-BETAS)/2;
TETAXY=(TETAY+TETAZ+TETAS);
%%%%%%%%%%%%%%%%%%%%%%%%%%%%%%%%%%%%%%%%%%%%%%%%%%%%%%%%%%%%%%%%%%%%%%%%
TETA1= 15*(pi/180);
TETA2= 45*(pi/180);
TETA3= 45*(pi/180);
TETA4= 75*(pi/180);
TETA5= 90*(pi/180);
%%%%%%%%%%%%%%%%%%%%%%%%%%%%%%%%%%%%%%%%%%%%%%%%%%%%%%%%%%%%%%%%%%%%%%%%
TETAON = 10* (pi/180);
TETAOFF = 37* (pi/180);
TETAQ = 60* (pi/180);
%%%%%%%%%%%%%%%%%%%%%%%%%%%%%%%%%%%%%%%%%%%%%%%%%%%%%%%%%%%%%%%%%%%%%%%%
TETAIN = 20.1* (pi/180);      %Initial Rotor Position
V=150;                        %applied voltage
R=1.30;                        %Resistance of motor
J=0.0013;                     %Moment of Inertia
F=0.0183;                     %Frictional Coefficient
DELTAI = 0.5;                 % change in current
LMIN = 8e-3;                  %Minimum Inductance
LMAX = 60e-3;                 %Maximum Inductance

G= (inv([TETAX 1;TETAY 1]))*([LMIN;LMAX]);
AUP= G(1);
BUP =G(2);
H=(inv([(TETAY+TETAZ) 1; TETAXY 1]))*([LMAX;LMIN]);
ADOWN=H(1);
BDOWN=H(2);
DL=AUP;

```

Initialization for 6/4 Motor with unequal betas

```

BETAS = 24*(pi/180);      % angle of the arc of stator
BETAR = 36*(pi/180);      % angle of the arc of rotor
TETAS = (2*pi)*((1/NR)-(1/NS)); % Step angle per transition
%%%%%%%%%%%%%%%%%%%%%%%%%%%%%%%%%%%%%%%%%%%%%%%%%%%%%%%%%%%%%%%%%%%%%%%%
TETAX = (pi/NR) - ((BETAR+BETAS)/2);      % tetax = 15 degrees
TETAY = (pi/NR) - ((BETAR-BETAS)/2);      % tetay = 45 degrees
TETAZ = (BETAR-BETAS)/2;
TETAXY=(TETAY+TETAZ+TETAS);
%%%%%%%%%%%%%%%%%%%%%%%%%%%%%%%%%%%%%%%%%%%%%%%%%%%%%%%%%%%%%%%%%%%%%%%%
TETA1= 15*(pi/180);
TETA2= 39*(pi/180);
TETA3= 51*(pi/180);
TETA4= 75*(pi/180);
TETA5= 90*(pi/180);
%%%%%%%%%%%%%%%%%%%%%%%%%%%%%%%%%%%%%%%%%%%%%%%%%%%%%%%%%%%%%%%%%%%%%%%%
TETAON = 10* (pi/180);
TETAOFF = 35* (pi/180);
TETAQ = 60* (pi/180);
%%%%%%%%%%%%%%%%%%%%%%%%%%%%%%%%%%%%%%%%%%%%%%%%%%%%%%%%%%%%%%%%%%%%%%%%
G= (inv([TETAX 1;TETAY 1]))*([LMIN;LMAX]);
AUP= G(1);
BUP =G(2);

ADOWN = -AUP;
BDOWN = LMAX-ADOWN*(TETA3);
DL=AUP;
DLa=0;                                % no change in inductance during TETAZ

```


Initialization for 8/6 Motor with equal betas

```

NS=8;                                %No. of Stator Poles
NR=6;                                %No. of Rotor Poles
P=4;

TETAX = (pi/NR)-( (BETAR+BETAS)/2) ;% tetax = 15 degrees
TETAY = (pi/NR)-( (BETAR-BETAS)/2); % tetay = 45 degrees
TETAZ = (BETAR-BETAS)/2;
%TETAXY=(TETAY+TETAS) ;
TETAXY=(TETAY+TETAZ+TETAS);
%%%%%%%%%%%%%%%%%%%%%%%%%%%%%%%%%%%%%%%%%%%%%%%%%%%%%%%%%%%%%%%%%%%%%%%%
BETAS = 15*(pi/180);                  % angle of the arc of stator
BETAR = 15*(pi/180);                  %angle of the arc of rotor
TETAS = (2*pi)*((1/NR)-(1/NS));       % Step angle per transition
%%%%%%%%%%%%%%%%%%%%%%%%%%%%%%%%%%%%%%%%%%%%%%%%%%%%%%%%%%%%%%%%%%%%%%%%
TETA1= 15*(pi/180);
TETA2= 30*(pi/180);
TETA3= 30*(pi/180);
TETA4= 45*(pi/180);
TETA5= 60*(pi/180);
%%%%%%%%%%%%%%%%%%%%%%%%%%%%%%%%%%%%%%%%%%%%%%%%%%%%%%%%%%%%%%%%%%%%%%%%
TETAON = 5* (pi/180);
TETAOFF = 18* (pi/180);
TETAQ = 40* (pi/180);
%%%%%%%%%%%%%%%%%%%%%%%%%%%%%%%%%%%%%%%%%%%%%%%%%%%%%%%%%%%%%%%%%%%%%%%%
TETAON = 20.1* (pi/180); %Initial Rotor Position
V=280;                               ;%applied voltage
R=1.30;                               %Resistance of motor
J=0.0013;                             %Moment of Inertia
F=0.0183;                             %Frictional Coefficient
LMIN = 8e-3;                          %Minimum Inductance
LMAX = 60e-3;                         %Maximum Inductance

G= (inv([TETAX 1;TETAY 1]))*([LMIN;LMAX]);
AUP= G(1);                            %Slope furing Uprising of inductance
BUP =G(2);
H=(inv([ (TETAY+TETAZ) 1; TETAXY 1]))*([LMAX;LMIN]);
ADOWN=H(1);                           %Slope during decline of Inductance
BDOWN=H(2);
DL=AUP;

```